Andean Geology 42 (3): 285-312. September, 2015
doi: 10.5027/andgeoV42n3-a01

Andean Geology
www.andeangeology.cl

Detrital-zircon U-Pb geochronology of the Quebrada del Carrizo Metamorphic Complex and El Jardín Schists and spatially-related granitoids of the Sierra Castillo Batholith

Víctor Maksaev[1], Javier Arancibia[1], Francisco Munizaga[1], Colombo Tassinari[2]

[1] *Departamento de Geología, Universidad de Chile, Plaza Ercilla 803, casilla 13518, Correo 21, Santiago, Chile. vmaksaev@ing.uchile.cl; onegaiarthas@hotmail.com; fmunizag@ing.uchile.cl*

[2] *Instituto de Geociencias, Universidade de Sao Paulo, Rua do Lago, 562-Cidade Universitária CEP 05508-080, Sao Paulo, Brasil. ccgtassi@usp.br*

ABSTRACT. U-Pb detrital-zircon geochronology of two discrete outcrops of mica schists of the western border of the Domeyko Cordillera in the Region of Atacama, northern Chile, indicates that the maximum age of sedimentation of their protolith corresponds to the Late Carboniferous to Early Permian. The Early Permian granitoids of the Sierra Castillo Batholith that intruded the metamorphic rocks show ductile deformation and were emplaced within hot crust not much later than the greenschist-facies metamorphism peak that affected their host rocks. Therefore, the metamorphism of the Quebrada del Carrizo Metamorphic Complex and El Jardín Schists is constrained temporarily between the maximum age of sedimentation of detrital zircons (314±11 to 291±5 Ma) and the crystallization of Early Permian intrusions (292.2±6.6 to 278.3±5.8 Ma), thus pointing to Early Permian metamorphic peak. Concentration of U-Pb ages between 400 and 600 Ma indicate eastern detrital input sources, such as the Pampean and Brasiliano orogenies and the Ordovician-Silurian Famatinian magmatic arc of northwestern Argentina. Other concentration of detrital-zircon U-Pb ages between 900 to 1,200 Ma reflect contributions of magmatic rocks of age of the Proterozoic Sunsas orogeny (Grenville). Whereas, only few grains of zircon with U-Pb ages older than 1,200 Ma occur and these may correspond to a minor contribution zircon from South American cratonic areas. Zircon grains of Devonian age are scarce in populations of zircons analyzed, consistent with a passive margin and a lull of magmatic activity during this period in the paleo-Pacific border of Gondwana. The U-Pb detrital zircon data from the Quebrada del Carrizo Metamorphic Complex and El Jardín Schists coincide with detrital-zircon U-Pb data previously published for other metamorphic complexes of central-northern Chile, which are part of a Late Paleozoic subduction complex or accretionary wedge developed in the western edge of Gondwana. Consequently, the Quebrada del Carrizo Metamorphic Complex and El Jardín Schists are relics of the same Paleozoic accretionary wedge, which constituted the substratum for the emplacement of the Permian plutons of the Sierra Castillo Batholith.

Keywords: Geochronology, U-Pb dating, Detrital zircon, Gondwana, Paleozoic, Carboniferous, Permian, Metamorphic rocks, Atacama.

RESUMEN. Geocronología U-Pb de circones detríticos del Complejo Metamórfico Quebrada del Carrizo y Esquistos El Jardín y granitoides espacialmente relacionados del Batolito Sierra Castillo. Dataciones U-Pb de circones detríticos de dos afloramientos de esquistos micáceos del borde oeste de la cordillera de Domeyko en la Región de Atacama, norte de Chile, indican que la edad máxima de sedimentación de su protolito corresponde al Carbonífero Tardío-Pérmico Temprano. Los granitoides del Pérmico Temprano del Batolito Sierra Castillo situados en los esquistos muestran deformación dúctil y probablemente se emplazaron en corteza caliente, no mucho más tarde que el máximo de metamorfismo de facies de esquistos verdes que afectó a sus rocas de caja. Por lo tanto, el metamorfismo de las rocas del Complejo Metamórfico Quebrada del Carrizo y los Esquistos El Jardín está ubicado temporalmente entre el Carbonífero Tardío-Pérmico Temprano que es la edad máxima de sedimentación de circones detríticos (314±11 a 291±5 Ma) y la edad de cristalización de intrusivos del Pérmico Temprano (292,2±6,6 a 278,3±5,8 Ma), consecuentemente indicando un máximo metamórfico del Pérmico Temprano. Las concentraciones de edades U-Pb entre 400 y 600 Ma indican aporte de detritos de fuentes orientales como las orogenias Brasiliana y Pampeana y del arco magmático Famatiniano del Ordovícico-Silúrico del noroeste de Argentina. Otras concentraciones de edades U-Pb de 900 a 1.200 Ma reflejan aportes de rocas magmáticas de la edad de la orogenia Sunsas (Grenville) del Proterozoico, mientras que hay solo escasos granos de circón con edades U-Pb mayores de 1.200 Ma y estos pueden corresponder a un aporte menor de zonas cratónicas sudamericanas. Los granos de circones de edad devónica son escasos en las poblaciones de circones analizadas, en consonancia con un margen pasivo y una pausa de la actividad magmática durante este período en el borde paleo-Pacífico de Gondwana. Los datos U-Pb de circones detríticos del Complejo Metamórfico Quebrada del Carrizo y los Esquistos El Jardín son coincidentes con datos U-Pb de circones detríticos publicados anteriormente para otros complejos metamórficos del centro-norte de Chile, los que son parte de un complejo de subducción Paleozoico Tardío o cuña de acreción desarrollado en la borde occidental de Gondwana. Por lo tanto, el Complejo Metamórfico Quebrada del Carrizo y los Esquistos El Jardín son relictos de la misma cuña de acreción del Paleozoico Tardío, la que constituyó el sustrato donde se emplazaron los plutones del Pérmico Temprano del Batolito Sierra Castillo.

Palabras clave: Geocronología, Datación U-Pb, Circones detríticos, Gondwana, Paleozoico, Carbonífero, Pérmico, Rocas metamórficas, Atacama.

1. Introduction

We have investigated the U-Pb detrital-zircon geochronology for two discrete outcrops of metamorphic rocks of sedimentary protolith that are present in the western border of the Domeyko Cordillera in the Atacama Region of northern Chile. These are the Quebrada del Carrizo Metamorphic Complex (Cornejo *et al.,* 2009) and El Jardín Schists (Tomlinson *et al.,* 1999), respectively (Fig. 1), which are relics of the host rocks of the composite Permian Sierra Castillo Batholith, exposed east of El Salvador, northern Chile (Tomlinson *et al.,* 1999; Cornejo *et al.,* 2009). We aim to determine the maximum age of sedimentation of detrital zircons, the provenance of the detrital deposits that constitute the protolith of the micaceous schists, and their regional geological significance. In addition, we also provide U-Pb dates for igneous zircons from granitoids emplaced within the metamorphic rocks to constrain the minimum age of metamorphism. The studied metamorphic rocks are exposed in the Jardín and del Carrizo creeks, in relatively small areas (<0.25 km^2) which occur on the border of the eastern block of the Sierra Castillo thrust fault (cf. Perelló and Müller, 1984; Tomlinson *et al.,* 1993, 1999; Cornejo *et al.,* 1993, 2009) and are bounded to the west by this sub-vertical, east-dipping, regional fault that extends along the western flank of the Cordillera de Domeyko in the northern portion of the Atacama Region (Perelló and Müller, 1984; Tomlinson *et al.,* 1999) (Fig. 1).

The first description of the metamorphic rocks exposed in the Jardín creek (or lower Asientos creek) was published by García (1967), referred to as "Mica esquistos de Quebrada Asientos". Later the same unit was described as a "Metamorphic Complex" by Pérez (1982) and Perelló and Müller (1984), and then renamed as "El Jardín Schists" by Tomlinson *et al.* (1999). While, the metamorphic rocks exposed in the del Carrizo creek about 54 km farther north, were described by Cornejo *et al.* (1993) as "Quebrada del Carrizo Metamorphic Complex", a further structural study was completed by Niemeyer (1999), and a more recent description published by Cornejo *et al.* (2009).

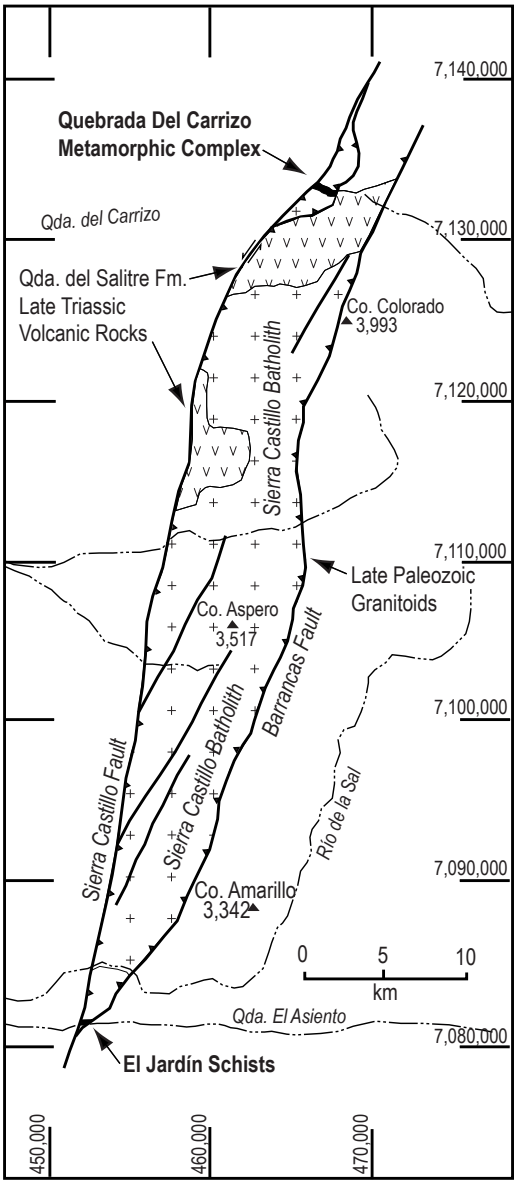

FIG. 1. Schematic geological setting of the Quebrada del Carrizo Metamorphic Complex and the El Jardín Schists relative to the Late Paleozoic, fault-bounded Sierra Castillo Batholith. Modified after Niemeyer, 1999, Tomlinson *et al.,* 1999, and Cornejo *et al.,* 2009.

2. Quebrada del Carrizo Metamorphic Complex and El Jardín Schists

The metamorphic rocks at the del Carrizo creek are exposed on the both flanks of the east-west-trending canyon-valley (Figs. 2 and 3), under a flat cover of Miocene welded tuffs (Llano Las Vicuñas ignimbrites; Cornejo *et al.,* 2009), and overlying Upper Miocene to Pliocene alluvial gravels (Atacama Gravels; Cornejo *et al.,* 2009).

The Quebrada del Carrizo Metamorphic Complex include gray-colored mica schists and actinolite-rich greenschists; the mica schists are muscovite-bearing with variable amounts of granoblastic bands of quartz and albite that alternate with lepidoblastic muscovite-rich bands and less abundant chlorite. The greenschists show a subparallel foliation of actinolite with albite and scapolite porphyroblasts in a nematoblastic matrix of actinolite with biotite and epidote; interstitial titanite and opaque minerals; a mafic volcanic protolith is inferred for these rocks based on their mineralogy. The greenschists occur as massive dark greenish gray outcrops, but display a distinct greenish light blue color in enclaves of these rocks within granite or near contacts with the intrusion, due to a pervasive chloritization of the amphiboles.

The schists of Quebrada del Carrizo in part occur as enclaves within sheared, medium-grained granite and are bounded by the east-dipping Sierra del Castillo thrust fault to the west and by another west-dipping thrust fault to the east (Fig. 2). These

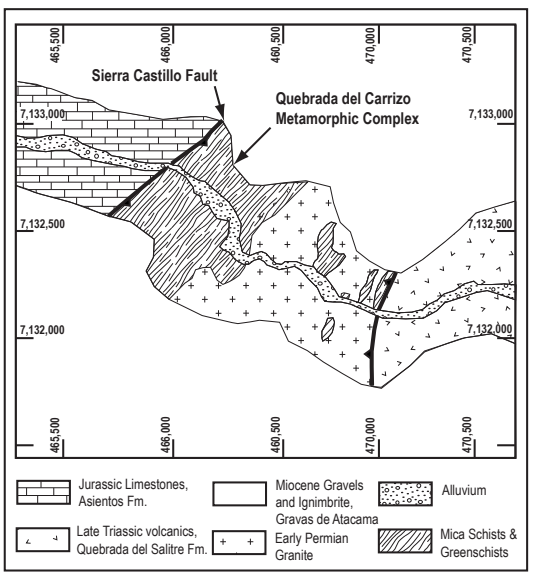

FIG. 2. Geological map of the Quebrada del Carrizo metamorphic complex (base topography after Google Earth image; lithostratigrapic units after Cornejo *et al.,* 2009).

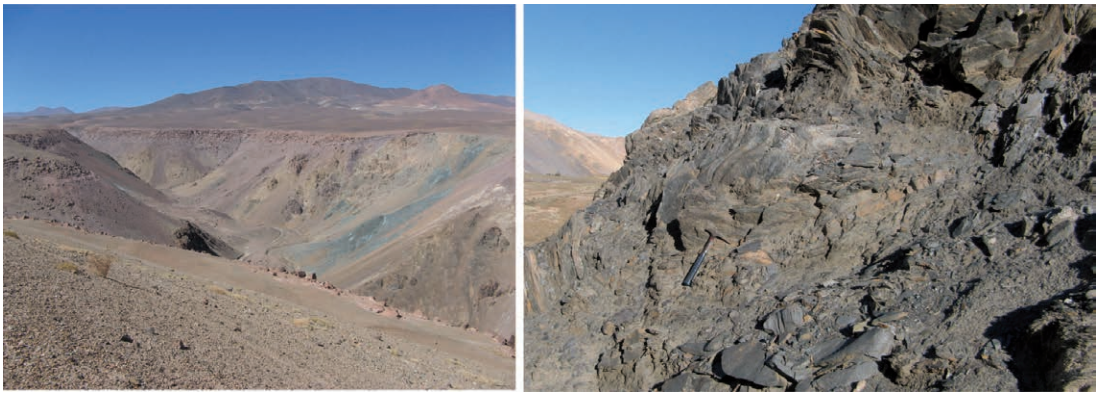

FIG. 3. Quebrada del Carrizo metamorphic complex: (left) general view (to the SE) of the outcrops in the del Carrizo creek underlying Miocene ignimbrite and gravels, (right) local appearance of folded mica schists (view to the W).

faults have been interpreted by Niemeyer (1999) as forming a sinistral, transpressive, tectonic wedge developed during the Eocene-Oligocene. The schists of the Quebrada del Carrizo are deformed into isoclinal folds with superimposed asymmetric folds and crenulation with fold axis near parallel with the main foliation that strikes NE and dips from 35° to 70° to the east.

The El Jardín Schists correspond to metamorphic rocks that are exposed in the northern flank of the Jardín creek (or lower Asientos creek) within a structural wedge formed by the southward convergence of the east-dipping Sierra Castillo thrust fault and the west-dipping Barrancas thrust fault (cf. Perelló and Müller, 1984; Tomlinson *et al.,* 1999) and under a 250 m thick, flat cover of Miocene alluvial gravels with minor volcanic ash intercalations (Atacama Gravels; Tomlinson *et al.,* 1999) (Fig. 4).

The metamorphic rocks are gray-colored, mica schists, with a main foliation striking N20-30° E and dipping from 25° to 50° to the west, which have superimposed asymmetrical folds with semiperpendicular axis strike direction and local crenulation cleavage (kink bands) with wavelength less than 3 cm (Fig. 5). There are 2 to 5 cm thick segregation quartz veins and heterogeneity in the grain size, with protruding quartz-rich, coarser-grained layers that are more resistant to weathering, which alternate with mica-rich fine-grained levels that are friable and more weathered (Fig. 5).

The schists have granoblastic texture when quartz is the dominant phase over micas, whereas lepidoblastic textures characterize the more micaceous

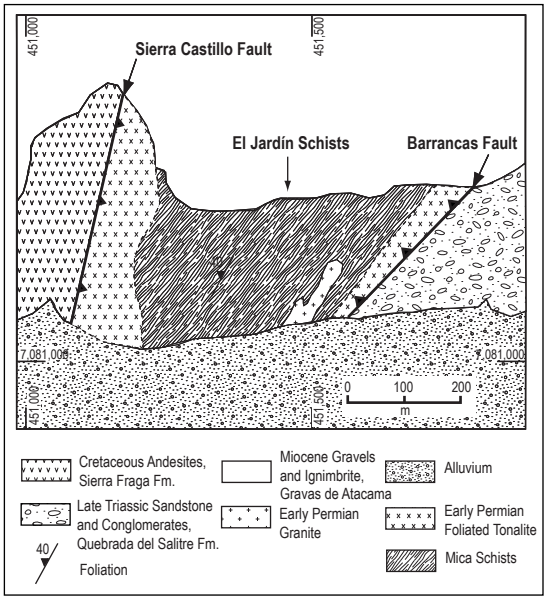

FIG. 4. Geological map of the El Jardín Schists (base topography after Google Earth image; lithostratigrapic units after Tomlinson *et al.,* 1999).

metamorphic rocks. Poikiloblastic textures are less frequent with albite porphyroblasts with inclusions of fine grains of quartz, albite and white micas, plus some carbonaceous material. Bands formed of crystalline aggregate of quartz alternate with muscovite-rich or chlorite bands, and when present, albite porphyroblasts occur within the micaceous bands that are deformed on the edges of the larger albite grains. Chlorite and opaque minerals occur

FIG. 5. El Jardín Schists: (left) general appearance of the outcrops, (right) crenulation cleavage in the mica schists.

in some samples, which appear to have completely replaced biotite; also there are late calcite veinlets.

The mineral assemblage of actinolite±albite± chlorite±epidote±quartz of the greenschists and quartz±albite±muscovite±chlorite of the mica schists indicate that the protoliths of the two exposures (El Jardín and Quebrada del Carrizo) were subjected to greenschists facies metamorphism. The characteristics of the micaceous schists are consistent with a sedimentary protolith, which is corroborated by rounded to subrounded zircon grains separated from these rocks, some of which have graphitic coatings (Fig. 6).

Local light pink, granitic injections occur within fold hinges of the El Jardín Schists and a dark green, foliated tonalite is intruded crosscutting the schist foliation, these granitoids are part of the southern end of the Sierra Castillo Batholith, exposed mostly to the north, along the Domeyko Cordillera east of El Salvador (Tomlinson *et al.,* 1999) (Figs. 1 and 4).

The granite intruded within a fold hinge in the Jardín Schists (CHY-74; Fig. 7) is medium-grained, leucocratic rock with hypidiomorphic granular texture and composed of quartz, plagioclase and orthoclase, with less than 10% of chlorite, muscovite, and opaque minerals that appear to have completely replaced biotite. The quartz grains show undulatory extinction and subgrains, some plagioclase are bent and show wedge twins, but also microfractures, indicating ductile and fragile deformations of the granite. The tonalite (CHY-19a) is a medium-grained, mesocratic rock with hypidiomorphic granular texture and composed mainly by plagioclase and hornblende and minor biotite and quartz; it has a foliation defined by preferential orientation of tabular minerals (Fig. 7). The quartz grains show undulatory extinction and plagioclase grains have wedge twins and microfractures, indicating also ductile and fragile deformation of the tonalite.

The sheared granite (CHY-83) that crosscuts the metamorphic rocks at the del Carrizo creek is composed of rounded and partly corroded grains of quartz, orthoclase, and plagioclase with deformation twins, and minor chloritized biotite, within a felsitic microcrystalline groundmass composed of quartz, plagioclase and muscovite. Wedge twins, recrystallization and microfractures of the minerals evidence ductile and fragile deformation of this granite.

3. Previous geochronological data

A whole rock K-Ar age of 196±5 Ma was reported for mica schist by Cornejo *et al.* (1993) and a muscovite K-Ar age of 278±6 Ma by Tomlinson *et al.* (1999) for an amphibole, scapolite and muscovite schist of the Jardín Schists. In addition, Tomlinson *et al.* (1999) reported a sericite K-Ar age of 264±6 Ma for muscovite-bearing granite body that crosscut these metamorphic rocks. Besides, a whole-rock K-Ar age of about 151 Ma was originally reported for the Quebrada del Carrizo Metamorphic Complex by Cornejo and Mpodozis (1996), but later Cornejo *et al.* (2009) published a muscovite K-Ar age of 272±6 Ma for a mica schist, a biotite K-Ar age of 269±6 Ma for a biotite and

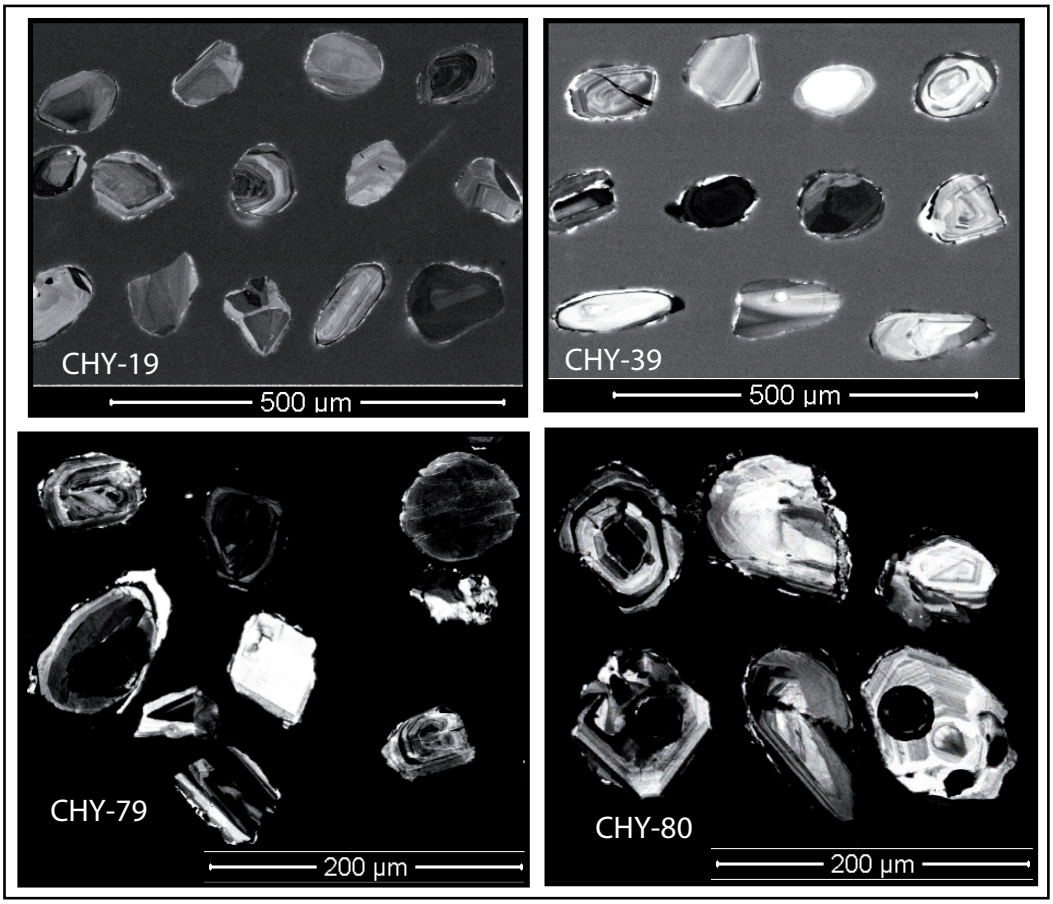

FIG. 6. Cathodoluminiscence images of detrital zircon grains from the dated samples of schists; note the internal zoning typical of igneous zircon, but the rounded shape of the grains due to wear during sediment transport. Black circles in the lower images are laser beam pits. Upper images from Centro de Pesquisas Geocronológicas, Brazil and lower images from the laboratory of the Universidad de Chile.

FIG. 7. Intrusions into the El Jardín Schists: (left) contact between schists and granite emplaced within a fold hinge, (right) aspect of the foliated tonalite.

amphibole schist and an amphibole $^{40}Ar/^{39}Ar$ age of 277±6 Ma for an arfvedsonite and scapolite schist. While, there are a number of Permian K-Ar dates that range from 281±6 to 254±8 Ma for the granitic rocks of the Sierra Castillo Batholith (Tomlinson *et al.,* 1999; Cornejo *et al.,* 2009) and Rb-Sr isochrones of 278±4, 270±10 and 269±4 Ma (Halpern, 1978; Brook *et al.,* 1986).

The published K-Ar and $^{40}Ar/^{39}Ar$ data for the Jardín and Quebrada del Carrizo metamorphic rocks clearly indicate their Early Permian minimum age, but the actual age of the protolith remained indefinite, just as any actual correlation of these metamorphic rocks with other units and their significance in the regional geological context.

4. Analytical methods

Zircon grains were obtained from rock samples following normal mineral separation procedures at the Geology Department, University of Chile, which included crushing, washing, and heavy liquid and magnetic separation. Zircon grains were mounted in epoxy and later polished. The zircon mounts were cleaned with 3% HNO_3 and later washed in ultraclean water and cathodoluminescence (CL) images were prepared for all samples prior to U-Pb analyses.

U-Pb analyses were performed at the Isotope Geochemistry laboratory, in the Andean Geothermal Center of Excellence, Department of Geology of the Universidad de Chile. Analyses were performed using a Photon Machines Analyte G2 192 nm ArF excimer laser ablation system with a HelEx 2 ablation cell, coupled to a Thermo Scientific Neptune Plus multicollector ICP-MS. The laser system is normally operated at 7-8 Hz with an ablation diameter of 25-30 μm. In order to reduce elemental fractionation and maximize the sensitivity, the ablated material is carried in helium gas (0.5 l/min) prior to entering the ICP torch (Günther *et al.,* 1999). The plasma conditions for U-Pb geochronology are typically 1200 W. Faraday cup detectors and ion counters are used simultaneously in static mode to measure ^{202}Hg, ^{204}Hg+^{204}Pb, ^{206}Pb, ^{207}Pb, ^{208}Pb, ^{235}U, ^{232}Th and ^{238}U. Data are collected with an integration time of 1.084 s per cycle. The ablation time is about 50 s which is equivalent to 50 cycles. The first 10 cycles are not used in the data reduction (pre-ablation) to achieve better signal stability and to eliminate surface contamination.

The measure sequence among standard -sample is 3 standards followed by 4 unknowns. A 20s blank is taken between every ablation. Normalization was carried out using the Plesovice zircon standard (337.13±0.37 Ma; Slama *et al.,* 2008) as primary standard, and SL2 or 91500 as secondary standard. The ^{238}U intensity and the $^{206}Pb/^{238}U$, $^{207}Pb/^{235}U$, $^{206}Pb/^{208}Pb$ ratios are recorded every session and are compared with the values reported in the literature. For the data reduction we use the Iolite software (Paton *et al.,* 2011), which allows to correct for downhole fractionation and choose the type of spline used to correct for instrument bias. Age calculation and plots were made using ISOPLOT software (Ludwig, 2003).

U-Pb analyses for sample CHY-39 were also performed by the Laser Ablation Inductively Coupled Plasma Mass Spectrometry (LA-ICP-MS) with a high-resolution, multiple collector mass spectrometer with a plasma source (MC-ICP-MS; Finnigan, Neptune), connected to an Excimer ArF laser (λ=193 nm) in the Geochronological Research Center (Centro de Pesquisas Geocronológicas) of the Sao Paulo University in Brazil. The ablated material was carried by Ar (~7 l/min), and He (~0.6 l/min) in analyses of 60 cycles of 1 second. The measure sequence among standard, blank and unknown was: 2 blanks, 3 standards, 13 unknowns, 2 blanks and 2 standards All analyses were conducted in static mode with a laser beam diameter of ~29 μm, operated with an output energy of 6 mJ and a pulse rate of 6 Hz. Normalization was carried out using Temora standard zircon (416.75±0.24 Ma, 95% confidence limits; Black *et al.,* 2003) and age calculation were performed using ISOPLOT V3 (Ludwig, 2003). Corrections for common Pb were applied to samples with $^{206}Pb/^{204}Pb$ lower than 1000, using Stacey and Kramers (1975) model at the age of crystallization and for polarization displacement. U-Pb data were plotted using ISOPLOT V3 (Ludwig, 2003). Errors for isotopic ratios are presented at ±1σ level in Appendix 1a and 1b.

The U-Pb age for the tonalite sample CHY-19a was obtained using a sensitive high resolution ion microprobe (SHRIMP II) in the Geochronological Research Center (Centro de Pesquisas Geocronológicas) of the Sao Paulo University in Brazil, following the procedures described by Maksaev *et al.* (2014).

Interpreted ages are based on $^{206}Pb/^{238}U$ for <1.0 Ga grains and on $^{206}Pb/^{207}Pb$ for >1.0 Ga grains.

U-Pb analyses that were >30% discordant or >5% reverse discordant were excluded from interpretations and the respective concordia plots are shown in figure 8. Sample location and analytical U-Pb data is included in Appendix 1a for detrital-zircon and 1b for igneous zircon grains. The numerical ages are assigned to the International Stratigraphic Chart of the International Commission on Stratigraphy (Cohen *et al.,* 2013).

5. Results

Sample CHY-79; Quebrada del Carrizo Metamorphic Complex: lepidogranoblastic albite-quartz-muscovite schist (Fig. 9a) composed of 35% anhedral albite (0.5 to 1.5 mm long), 30% anhedral quartz (0.1 to 1.0 mm), 30% subhedral deformed muscovite (0.1 to 0.5 mm long), 10% opaque minerals, traces of epidote and tourmaline. 40 U-Pb ages were used from 61 individual grains analyzed (20 discarded). The largest group of zircon U-Pb ages is from 405 to 560 Ma (n=17; peak at 470 Ma; Fig. 10) that represent 42.5% , followed by the youngest population from 271 to 317 Ma (n=10; peak at 303 Ma) that represents 25%; other smaller groups are from 615 to 680 (n=4; peak at 650 Ma; 10%); from 790 to 841 (n=4; peak at 840; 10%), and from 1098 to 1,163 Ma (n=4; peak at 1,130 Ma; 10%; Fig. 10).

Sample CHY-80; Quebrada del Carrizo Metamorphic Complex: lepidogranoblastic quartz-albite-chlorite schist (Fig. 9b) composed of 60% anhedral quartz (0.5 to 1.5 mm long), 18% anhedral albite (0.1 to 0.9 mm), 10% subhedral chlorite (0.1 to 0.5 mm long), 10% opaque minerals (0.1 to 0.3 mm), minor muscovite and calcite. 54 U-Pb ages were used from 69 individual grains analyzed (15 rejected).

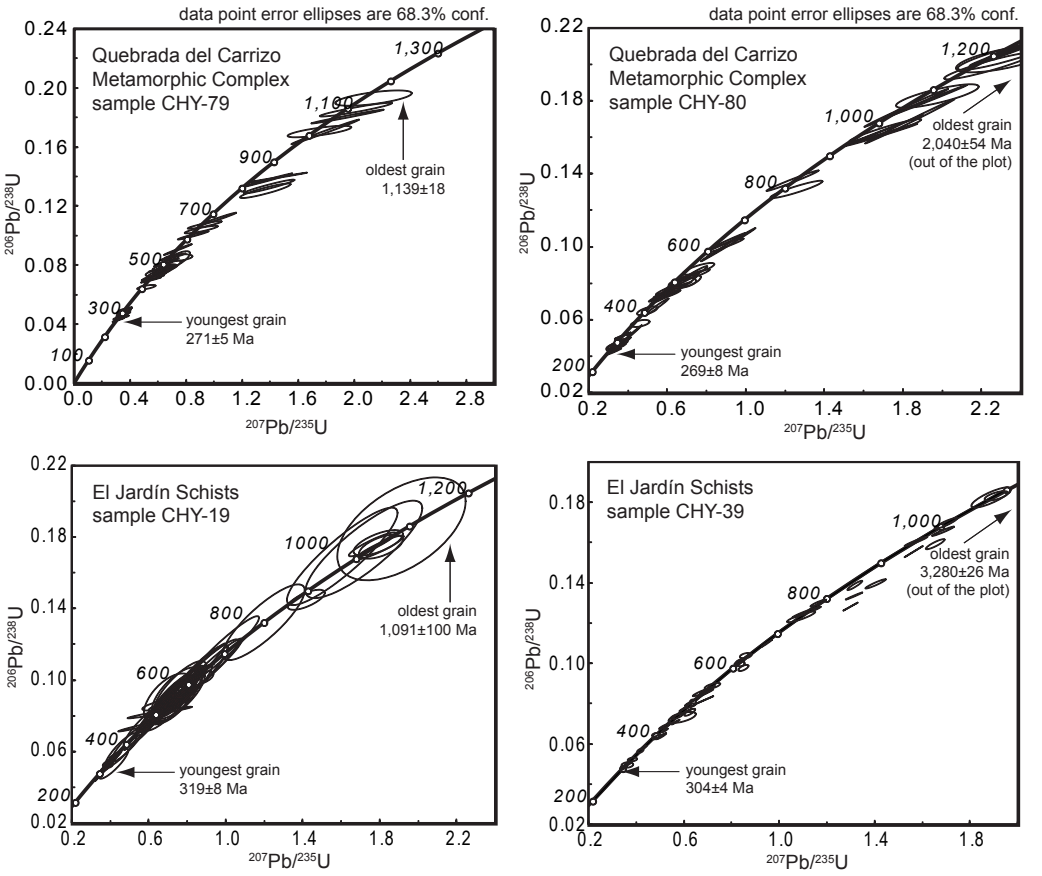

FIG. 8. Concordia diagrams of the analyzed samples of mica schist (discordant analyses excluded). Ages of oldest and youngest zircon grains are given in each plot.

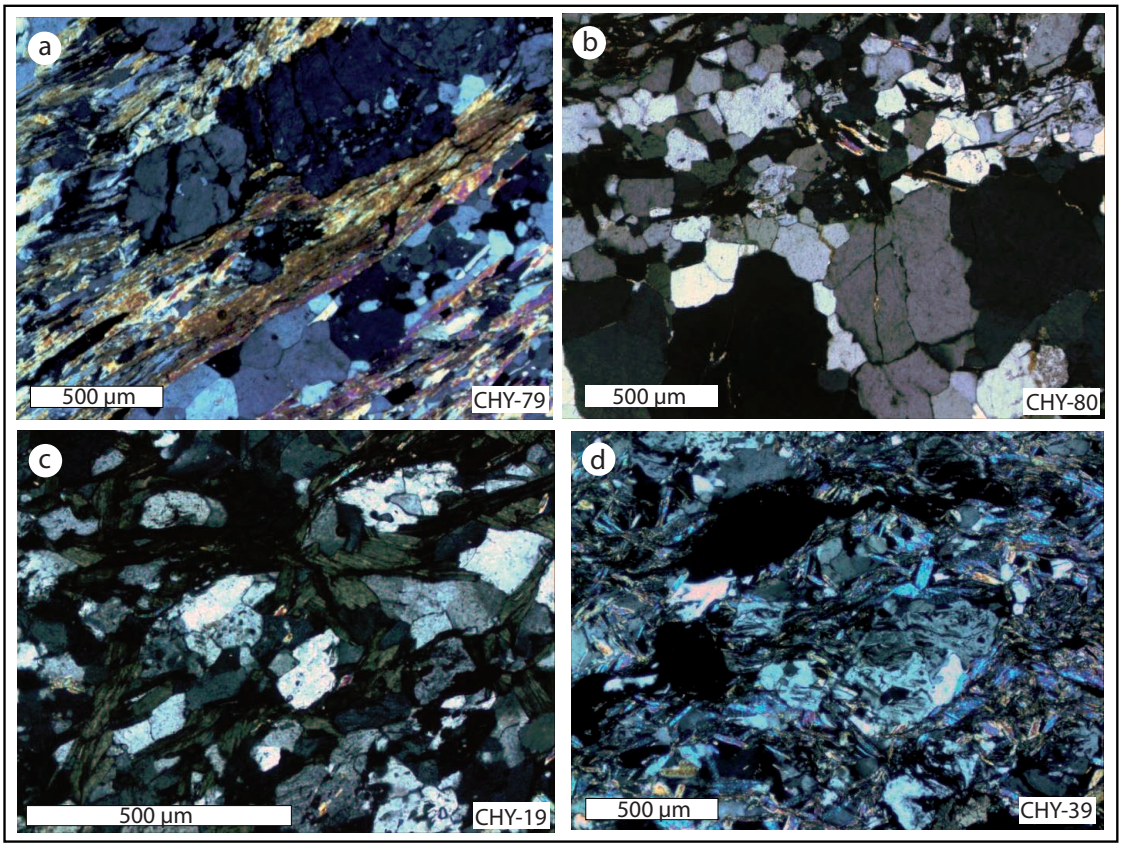

FIG. 9. Microphotographs (cross-polarized light) of samples of metamorphic rocks: **a.** CHY-79: albite-quartz-muscovite schist; **b.** CHY-80: quartz-albite-chlorite schist; **c.** CHY-19: albite-quartz-chlorite schist; and **d.** CHY-39: albite-quartz-muscovite schist.

The youngest group of zircon U-Pb ages from 269 to 321 is the largest one (n=18; peak at 292 Ma; Fig. 10) and represents 33.3%, followed by a population from 405 to 544 Ma (n=13; peak at 470 Ma) that represents 24%, and a group from 966 to 1,237 (n=11; peaks at 970 and 1,200 Ma) that represents 20.4%; a smaller group from 618 to 628 (n=3; peak at 620 Ma) represents 5.5% (Fig. 10).

Sample CHY-19; El Jardín Schists: lepidogranoblastic albite-quartz-chlorite schist (Fig. 9c) composed of 37% of anhedral albite (0.05 to 1.0 mm long), 35% anhedral quartz grains (0.1 to 0.5 mm), 25% subhedral chlorite (0.1 to 0.5 mm long), 2% muscovite and 1% opaque minerals. 59 U-Pb ages were used from 71 individual grains analyzed (12 discarded). The largest group of zircon U-Pb ages is from 460 to 716 Ma (n=41; peak at 540 Ma with a secondary peak at 480 Ma; Fig. 10) that represents 69.4%, followed by group from 1,006 to 1,092 Ma (n=7; peak at 1,060 Ma) that represents 11.9%. The youngest group is from 319 to 336 Ma (peak at 331 Ma) that represent 8.5% (Fig. 10).

Sample CHY-39; El Jardín Schists: lepidogranoblastic albite-quartz-muscovite schist (Fig. 9d) composed of 35% anhedral albite (0.5 to 1.0 mm long), 28% anhedral quartz (0.1 to 1.5 mm), 20% subhedral muscovite (0.1 to 0.3 mm long), 15% subhedral chlorite, minor calcite and tourmaline. 56 U-Pb ages were used from 65 individual grains analyzed (9 discarded). The largest group of zircon U-Pb ages is from 401 to 673 Ma (n=24; peak at 530 Ma with a secondary peak at 480 Ma; Fig. 10) that represents 42.9%, followed by a population from 749 to 842 Ma (n=7; peaks at 800 Ma) that represents 12.5%; another group from 1,074 to 1,228 (n=6; peak at 1,080) that represents 10.7%; another

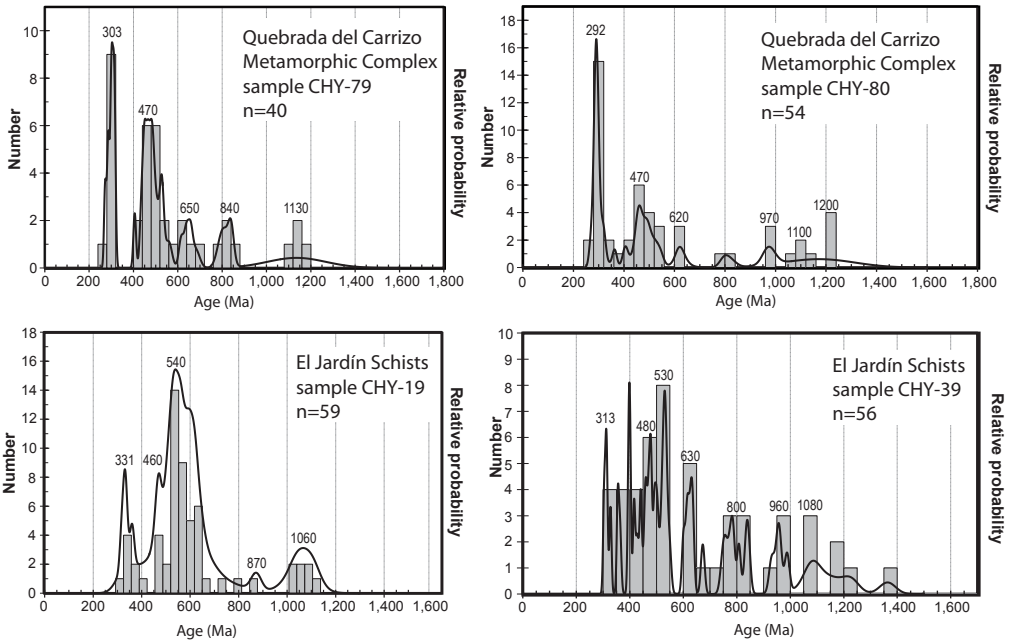

FIG. 10. U-Pb age histogram distribution of analyzed zircons (grey) with black probability curves from the mica schist samples. $^{238}U/^{206}Pb$ ages for all zircon <1 Ga were used and $^{207}Pb/^{206}Pb$ ages were used for all zircon grains >1 Ga (discordant analyses excluded).

population from 931 to 988 Ma (n=4; peak at 960) that represents 7.1%, and; some individual zircon grains yielded U-Pb ages from 1,364 to 3,435 Ma. The youngest population is from 304 to 328 Ma (n=4; peak at 313) that represents 7.1% (Fig. 10).

Most of the analyzed zircon grains from the schists show regular internal zonation pattern characteristic of a magmatic origin (Corfu *et al.,* 2003) (Fig. 6) and 50% of the zircon grains have Th/U ratio values >0.5, which are consistent with composition of igneous zircons according to Hoskin and Schaltegger (2003). The complete Th/U ratio ranges from 0.04 to 2.15 (Fig. 11), so that near half of zircon grains cannot be unambiguously classified by their Th/U ratio (Fig. 11), but only two zircon grains have Th/U ratio of 0.04 that is consistent with metamorphic-melt zircon composition (Hoskin and Schaltegger, 2003), and these are of zircon grains that yielded Proterozoic U-Pb ages of 1,005 and 2,409 Ma, respectively.

The youngest U-Pb ages of zircon in populations of detrital zircon are commonly used to constrain maximum depositional ages of stratigraphic units (*e.g.,* Dickinson and Gehrels, 2009 and references therein), but there is lack of consensus about the methods to do so (Barbeau *et al.,* 2009). Thus, we use four alternate measures of the youngest age which vary from least to most statistically robust as follows: **(a)** youngest single grain age, **(b)** youngest graphic peak controlled by more than one grain age, **(c)** weighted mean age of the youngest three or more

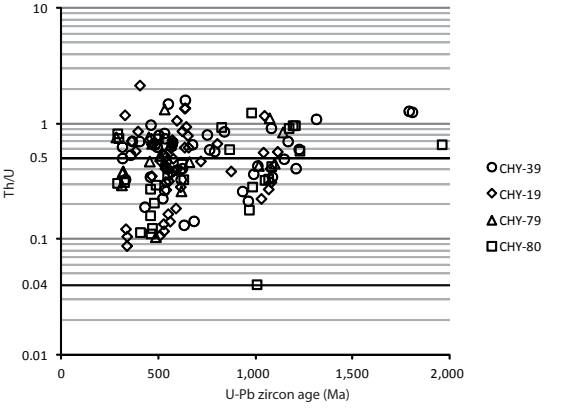

FIG. 11. Th/U ratio *versus* U-Pb zircon age plot of the analyzed zircon grains; the 0.004 and 0.5 black lines mark according to Hoskin and Schaltegger (2003) the upper and lower limits for zircon of metamorphic or magmatic origin, respectively.

grains that overlap at ±2σ **(d)** weighted mean age of all grains that correspond to the youngest peak (Table 1).

The maximum depositional age estimates of table 1 consistently correspond to Late Carboniferous for the El Jardín Schists and Early Permian for the Quebrada del Carrizo Metamorphic Complex; 314±11 Ma and 291±5 Ma, respectively, if the youngest most statistically robust values of table 1 are considered.

The U-Pb zircon ages obtained for intrusive rocks emplaced within the schists are of 278.3±5.8 Ma for granite (CHY-83) of the del Carrizo creek and of 285.7±6.8 for foliated tonalite (CHY-19a) of the Jardín creek (Fig. 12). A granite injection (CHY-74) within a fold hinge in the El Jardín Schists contains a group of inherited Neoproterozoic to Cambrian zircon grains (Fig. 12) that is analogous to the prominent maxima of U-Pb ages of the metamorphic rocks, thus probably incorporated from them. The youngest peak (5 spot analyses) defines a mean U-Pb age of 292.2±6.6 Ma for the granite (Fig. 12), which coincides within error limits with the age obtained for the foliated tonalite in the same area.

6. Discussion

The results of U-Pb dating of detrital zircons from four samples of mica schists are comparable to each other, as they show significant concentrations of U-Pb ages in the range of 400-600 Ma (Early Devonian to Late Proterozoic), which constitute the largest population in 3 of the samples, and define graphical relative probability peaks at 470 Ma for the zircon grains from the Quebrada del Carrizo and peaks at 460 and 480 Ma for those from El Jardín Schists (Fig. 10); the later also include higher peaks at 530-540 Ma (Fig. 10) with an ill-defined bimodal population. The four analyzed samples include youngest population of Late Paleozoic zircons, which are of ~269-321 Ma for Quebrada del Carrizo and of ~304-336 Ma for El Jardín Schists. Besides, the four samples include significant concentrations of U-Pb ages from 1,000 to 1,200 Ma, plus less prominent peaks centered at about 800 and 620-650. The overall coincidence of zircon grain age populations indicates a common provenance of the sedimentary material of the protolith of the mica schists of Quebrada del Carrizo Metamorphic Complex and El Jardín Schists.

The provenance of sedimentary material of other metamorphic complexes of central-northern Chile has been extensively discussed in previous studies (*e.g.,* Willner *et al.,* 2008; Bahlburg *et al.,* 2009; Álvarez *et al.,* 2011). These authors have shown that most of detritus have been derived from eastern sources, as U-Pb ages reflect input of zircon grains from all major orogenic cycles connected to the stepwise southwestward growth of the Amazonia craton in the southwestern Amazonia Orogenic System and the subsequent Terra Australis orogen between 2 Ga and 0.25 Ga, including additional input from the Arequipa Massif. Overall, the largest zircon contributions were derived from the Rondonia-San Ignacio, Sunsas, Famatinian and Late Paleozoic orogenic belts, with lesser input, in decreasing order of magnitude, from Brazilian-Pampean, Transamazonian and older Paleoproterozoic and Archean sources (Bahlburg *et al.,* 2009, and references therein). In our samples the youngest U-Pb age populations indicate detrital input from Late Paleozoic magmatism of the paleo-Pacific border of Gondwana (*e.g.,* Maksaev *et al.,* 2014), and the concentration of U-Pb ages within

TABLE 1. MAXIMUM DEPOSITIONAL AGE INTERPRETATIONS FROM YOUNGEST DETRITAL ZIRCON ANALYZED FROM EACH SAMPLE.

SAMPLE	Youngest single grain age	Graphical estimation	3 or more youngest grains overlapping U-Pb ages at ±2σ	Weighted mean age of the U-Pb data of the youngest peak
CHY-79	271±5	303	280±6 (n=3)	298±9 (n=10)
CHY-80	269±8	292	291±4 (n=15)	291±5 (n=19)
CHY-19	319±8	331	329±9 (n=5)	329±9 (n=5)
CHY-39	304±4	313	314±11 (n=4)	314±11 (n=4)

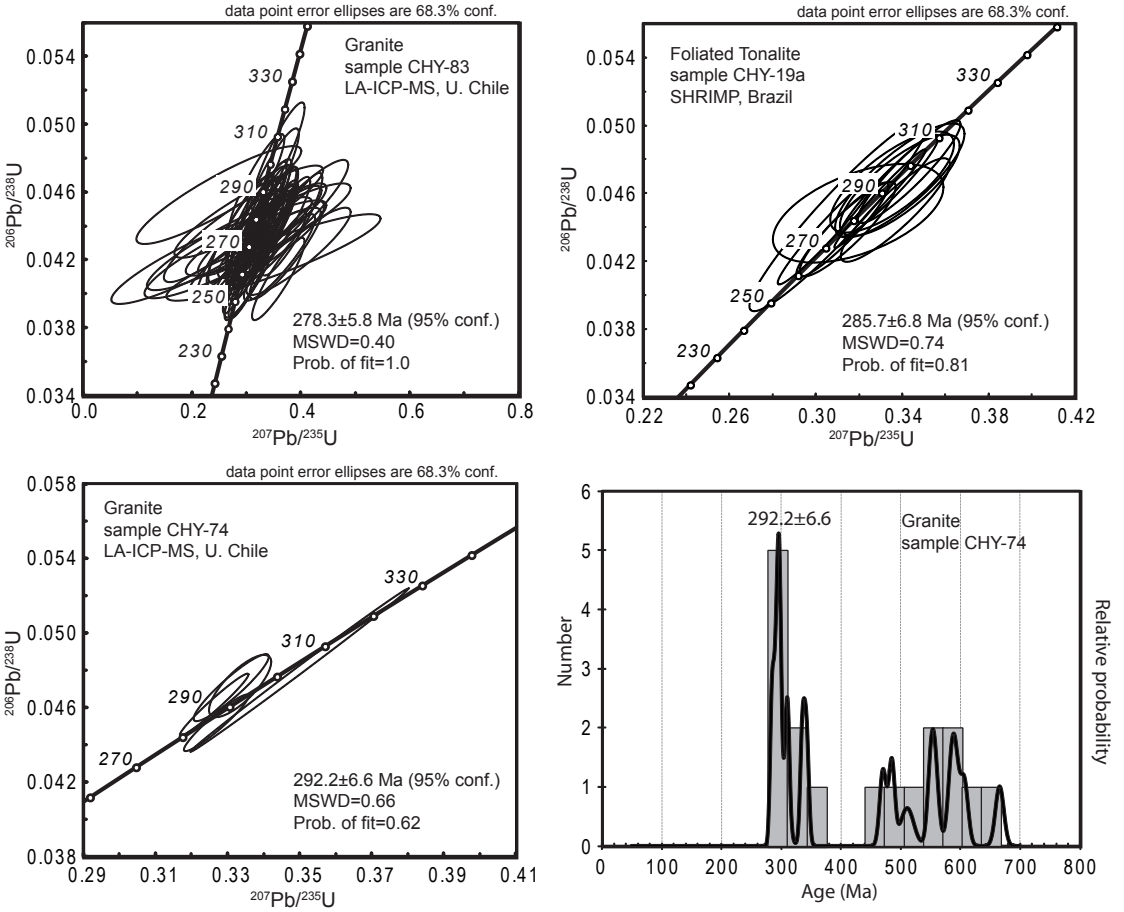

FIG. 12. Concordia diagrams of the analyzed samples of granitoids that were emplaced within the metamorphic rocks. The U-Pb age histogram distribution of analyzed zircons (grey) with black probability curves of the granite sample CHY-74 is also included to illustrate a population of inherited zircon grains.

the 400 to 600 Ma range imply contributions of the Famatinian and Pampean orogenies or the Braziliano cycle orogenesis. Although there is a larger proportion of Pampean age zircon grains in the Jardín Schists compared to those of the Quebrada del Carrizo Metamorphic Complex (Table 2). In addition, age concentrations between 900 and 1,200 Ma indicate a contribution of the Sunsas orogeny of the southwestern Amazonia margin of Grenville age (Bahlburg *et al.,* 2009, and references therein). Whereas there are scarce Devonian grains (Table 2), consistent with the development of a passive margin in this region and a lull of magmatic activity during this period (*e.g.,* Bahlburg *et al.,* 2009), and also only few zircon grains older than 1,200 Ma (Table 2).

Previously published detrital-zircon U-Pb data for other metamorphic rocks of northern Chile, such as: El Tránsito Metamorphic Complex, Huasco Metamorphic Complex, Choapa Metamorphic Complex, Las Tórtolas Formation and El Toco Formation (Willner *et al.,* 2008; Bahlburg *et al,* 2009; Álvarez *et al.,* 2011) (Fig. 13), are in agreement with our new detrital-zircon U-Pb data as they reveal eastern input of the Pampean and Famatinian or Braziliano orogenies, but also of Sunsas orogeny of Grenvillian age (Willner *et al.,* 2008; Bahlburg *et al.,* 2009; Álvarez *et al.,* 2011). In contrast, Late Paleozoic zircon grains are not always present, even in samples from the same metamorphic complex; for example Bahlburg *et al.* (2009) showed that 2 samples from Las Tórtolas Formation either have or

TABLE 2. PERCENTAGES OF U-Pb AGE DATES REPRESENTING KNOWN AND DISTINCT GEOCHRONOLOGICAL EVENTS IN PROBABLE SOURCE REGIONS ON THE AMAZONIA CRATON, THE AREQUIPA MASSIF AND THE CENTRAL ANDES.*

TIME INTERVAL (Ma)	EVENT	CHY-19 N=59 %	CHY-39 N=56 %	CHY-79 N=40 %	CHY-80 N=54 %
359-269	Late Paleozoic	8.5	9.9	25.0	35.2
420-359	Devonian (Late Famatinian)	5.1	8.9	2.5	5.5
520-420	Early Famatinian	10.2	19.6	32.5	18.5
650-520	Late Braziliano/Pampean	57.6	17.8	12.5	11.1
750-650	Early Braziliano	3.4	3.6	5.0	0.0
900-750	-	3.4	10.7	10.0	3.7
1,200-900	Sunsas Orogeny (Grenvillian)	11.9	14.3	12.5	16.7
2,000-1,200	-	0.0	12.5	0.0	7.4
>2000	-	0.0	3.6	0.0	1.9

* Temporal ranges of events according to Bahlburg *et al.* (2009 and references therein).

have not Late Paleozoic zircon grains, respectively. A similar situation is documented by the contrasting U-Pb data for samples from the El Tránsito Metamorphic Complex, east of Vallenar, obtained by Bahlburg *et al.* (2009) that show that a prominent maximum between 359 and 250 Ma (57%) with the youngest grain at 254±7 Ma and the data obtained by Álvarez *et al.* (2011) for the same metamorphic complex that lack of Late Paleozoic zircon grains.

The prominent maximum between 359 and 250 Ma of detrital-zircon U-Pb data for a mica schist of the El Tránsito Metamorphic Complex obtained by Bahlburg *et al.* (2009) has been questioned by Álvarez *et al.* (2011) and Salazar *et al.* (2013) due to the contrast with the U-Pb data of Alvarez *et al.* (2011) and the occurrence of Carboniferous rhyolitic tuffs of the Cerro Bayo Formation (U-Pb from 324.7±4.0 to 300.8±4.6 Ma; Salazar *et al.,* 2013; Maksaev *et al.,* 2014), which were thought to be deposited unconformably over the El Tránsito Metamorphic Complex. However, these Carboniferous rhyolitic rocks are actually in contact by a thrust fault with the metamorphic rocks (Salazar *et al.,* 2013), and this condition of very different crustal levels juxtaposed is not unique; for example, the high-pressure Limón Verde Metamorphic Complex in the Antofagasta Region of northern Chile, which have a maximum depositional age of 300 Ma and peak metamorphism dated at 280 Ma (Soto, 2013; Morandé, 2014), is in structural juxtaposition against penecontemporaneous supracrustal rhyolitic volcanic and sedimentary sequences of the Late Carboniferous to Early Permian Collahuasi Formation (Tomlinson and Blanco, 2008; Tomlinson *et al.,* 2012).

The Late Carboniferous to Early Permian maximum depositional age for the El Jardín Schists and Quebrada del Carrizo Metamorphic Complex are well in agreement with the maximum depositional age determined by Bahlburg *et al.* (2009) for the El Tránsito Metamorphic Complex, but also for Las Tórtolas Formation, Huasco Metamorphic Complex and Huentelauquén Formation. In addition, our U-Pb data are in agreement with the maximum depositional age determined by Álvarez *et al.* (2011) for the Choapa and Huasco metamorphic complexes and also with the maximum depositional age estimated by Willner *et al.* (2008) for the Choapa Metamorphic Complex (308 Ma), the Huentelauquén Formation (303 Ma) and coastal accretionary systems (344-308 Ma) of central Chile. Consequently, the incorporation of Late Paleozoic material is common-place in the protolith of the above mentioned metamorphic and metasedimentary rocks of north-central Chile (Fig. 13) and its absence in some samples reflect only variations in the input of these materials, rather than equivocal U-Pb data.

The U-Pb data for intrusions that were emplaced within the deformed metamorphic rocks of the Quebrada del Carrizo and El Jardín range from 292.2±6.6 to 278.3±5.8 Ma (Early Permian). The

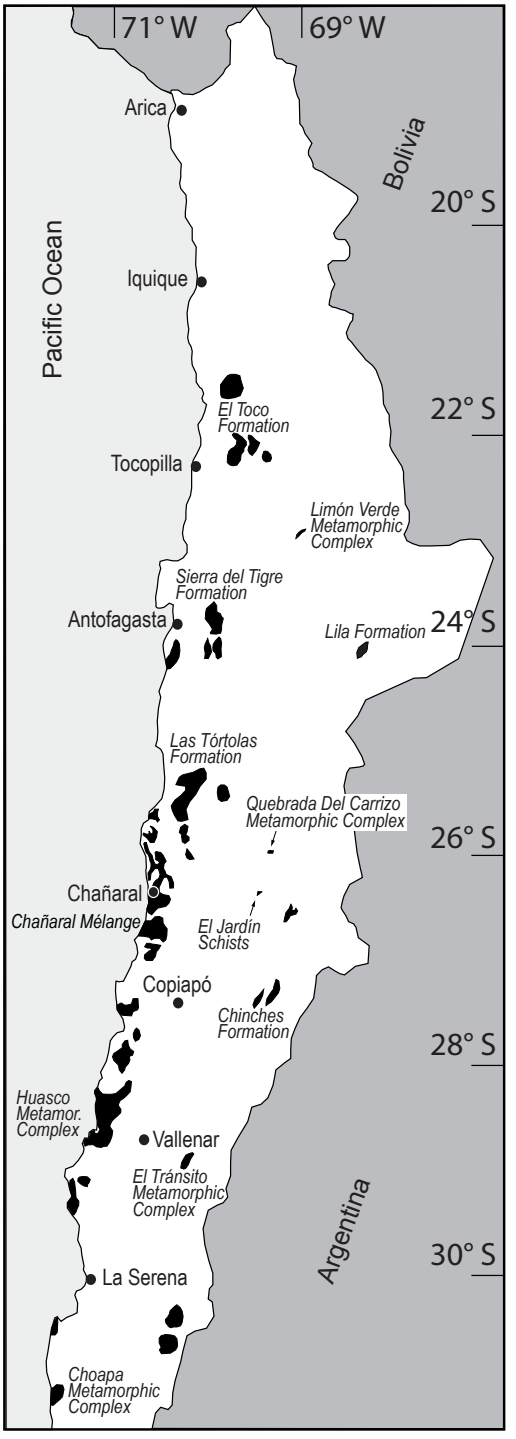

FIG. 13. Distribution of the Late Paleozoic metamorphic and sedimentary complexes of northern Chile (N of 32°S; modified after Hervé *et al.,* 2007) and location of the Quebrada del Carrizo Metamorphic Complex and El Jardín Schists.

zircon U-Pb age range obtained for the intrusive rocks is a bit older, but overlaps within error with the 278±6 to 269±6 Ma time-span indicated by a subset of the oldest previously published K-Ar and $^{40}Ar/^{39}Ar$ dates for the metamorphic rocks (Tomlinson *et al.,* 1999; Cornejo *et al.,* 2009), which obviously recorded only the minimum age of the latest thermal effect of the intrusions of the Sierra Castillo Batholith. It is worth mentioning that Perelló and Müller (1984) interpreted that the intrusions and the metamorphic rocks were part of the same intrusive complex that was affected by dynamic metamorphism related to the Cenozoic activity of the regional Sierra Castillo and Barrancas Faults. However, this interpretation is not supported by our new U-Pb data and is at variance with our and other author's geological observations (*e.g.,* Pérez, 1982; Tomlinson *et al.,* 1999; Cornejo *et al.,* 2009) that recognized the crosscutting relationship of the Permian intrusions in the metamorphic rocks.

The dated intrusive rocks have been affected by ductile deformation, but show no obvious evidence of metamorphism. Thus, the greenschists facies metamorphism is constrained between 291±5 and 278.3±5.8 Ma for the Quebrada del Carrizo Metamorphic Complex and between 314±11 and 292.2±6.6 Ma for El Jardín Schists, considering the respective maximum depositional age and the crystallization age of the granites; this point to Early Permian age for the metamorphic peak of the schists. The ductile deformation of the Early Permian granitoids suggests an emplacement within hot crust (relatively at a deep level), which probably took place not long after the greenschist facies, metamorphic peak of their country rocks, as further sustained by the closeness between the maximum depositional age for the schists and the crystallization ages of the intrusive rocks.

The Early Permian age of the greenschist facies peak metamorphism is somewhat younger, but may be assigned to the so called Toco orogeny; a metamorphic and plutonic event related to subduction of the paleo-Pacific or Panthalassian Ocean and the formation of an associated subduction complex or accretionary wedge on the edge of Gondwana, which was originally ascribed to the Early to Late Carboniferous (Bahlburg and Breitkreuz, 1991; Hervé *et al.,* 2007), but according to the U-Pb data should be extended to the Early Permian. It should be noted that the onset of late Paleozoic magmatism

in northern Chile occurred at *ca.* 330 Ma according to published U-Pb data (Maksaev *et al.,* 2014), thus the later stages of sedimentation, integration into the accretionary wedge, deformation and metamorphism of the studied rocks may overlap in time with the initial stages of the Late Paleozoic magmatism, represented by the Early Permian plutons of the Sierra Castillo Batholith, which were emplaced within the former accretionary wedge of the southwestern border of Gondwana.

7. Conclusions

Detrital-zircon U-Pb data from two discrete outcrops of mica schists in the Atacama Region of northern Chile indicate that the maximum depositional age of their protolith corresponds to the Late Carboniferous to Early Permian, indicating input of detritus from the Late Paleozoic magmatism of the western border of Gondwana. The Early Permian granitoids of the Sierra Castillo Batholith crosscut the schists and show ductile deformation, and probably were emplaced in hot crust, shortly after the greenschist facies metamorphic peak of their metamorphic country rocks. Therefore, the peak metamorphism for the Quebrada del Carrizo Metamorphic Complex and El Jardín Schists is constrained between the Carboniferous to Early Permian maximum depositional U-Pb ages of detrital zircon grains (314±11 and 291±5 Ma) and the crystallization of Early Permian intrusions (292.2±6.6 to 278.3±5.8 Ma).

The concentrations of detrital-zircon U-Pb ages within 400 and 600 Ma indicate significant detritus input from eastern sources including the Brazilian and Pampean Orogenies and the Ordovician to Silurian Famatinian magmatic arc of northwestern Argentina. Other concentrations of detrital-zircon U-Pb ages from 900 to 1,200 Ma are reflecting input from Sunsas (Grenville) age magmatic rocks, while only scarce U-Pb ages older than 1200 Ma occur and these may correspond to a minor input of zircon grains from South American cratonic areas. Grains of Devonian age are scarce in the analyzed zircon populations, consistent with a passive margin and lull of magmatic activity during this period on the paleo-Pacific border of Gondwana.

The detrital-zircon U-Pb data for the Quebrada del Carrizo Metamorphic Complex and El Jardín Schists are in agreement with detrital-zircon U-Pb data previously published for other metamorphic complexes of central-northern Chile, which are part of a Late Paleozoic subduction complex or accretionary wedge developed at the western border of Gondwana. Therefore, the El Jardín Schist and Quebrada del Carrizo metamorphic complex are relics of the same Late Paleozic accretionary wedge, where Early Permian plutons of the Sierra Castillo Batholith were emplaced.

Acknowledgements

This study was supported by CONICYT, Chile, through Fondecyt 1110093 grant to V. Maksaev and F. Munizaga (Universidad de Chile). We thank the analytic work of F. Barra of the Isotope Geochemistry laboratory of the Andean Geothermal Center of Excellence, Department of Geology of the Universidad de Chile and K. Sato of the Geochronological Research Center (Centro de Pesquisas Geocronológicas) of the Universidade de Sao Paulo, Brazil. Part of the data of this paper constituted the Bachelor´s Thesis of J. Arancibia. A review by Dr. J. Álvarez contributed to improve this paper.

References

Álvarez, J.; Mpodozis, C.; Arriagada, C.; Astini, R.; Morata, D.; Salazar, E.; Valencia, V.A.; Vervoort, J.D. 2011. Detrital zircons from late Paleozoic accretionary complexes in north-central Chile (28°-32°S): Possible fingerprints of the Chilenia terrane. Journal of South American Earth Sciences 32: 460-476.

Bahlburg, H.; Breitkreuz, C. 1991. Paleozoic evolution of active margin basins in the southern Central Andes (northwestern Argentina and northern Chile). Journal of South American Earth Sciences 4: 171-188.

Bahlburg, H.; Vervoort, J.D.; Du Frane, S.A.; Bock, B.; Augustsson, C.; Reimann, C. 2009. Timing of crust formation and recycling in accretionary orogens: Insights learned from the western margin of South America. Earth-Science Reviews 97: 227-253.

Barbeau Jr., D.L.; Olivero, E.B.; Swanson-Hysell, N.L.; Zahid, K.M.; Murray, K.E.; Gehrels, G.E. 2009. Detrital-zircon geochronology of the eastern Magallanes foreland basin: Implications for Eocene kinematics of the northern Scotia Arc and Drake Passage. Earth and Planetary Science Letters 284: 489-503.

Black, L.P.; Kamo, S.L.; Allen, C.M.; Aleinikoff, J.N.; Davis, D.W.; Korsch, R.J.; Foudoulis, C. 2003. TEMORA1: a new zircon standard for phanerozoic U-Pb geochronology. Chemical Geology 200: 155-170.

Brook, M.; Pankhurst, R.; Sheperd, T.; Shapiro, B. 1986. Andchron: Andean geochronology and metallogenesis. Overseas Development Administration, Open-file Report: 83 p. London.

Cohen, K.M.; Finney, S.; Gibbard, P.L.; Fan, J.-X. 2013 (updated). The ICS International Chronostratigraphic Chart. Episodes 36: 199-204.

Corfu, F.; Hanchar, J.M.; Hoskin, P.W.O.; Kinni, P. 2003. Atlas of zircon textures. Reviews in Mineralogy and Geochemistry 53: 469-500.

Cornejo, P.; Mpodozis, C. 1996. Geología de la Región de Sierra Exploradora (Cordillera de Domeyko 25°-26°S). Servicio Nacional de Geología y Minería, Informe Registrado IR-96-09: 330 p. Santiago.

Cornejo, P.; Mpodozis, C.; Ramírez, C.F.; Tomlinson, A.J. 1993. Estudio Geológico de la Región de Potrerillos y El Salvador (26°-27° Lat. S). Servicio Nacional de Geología y Minería-CODELCO, Informe Registrado, IR-93-01: 258 p. Santiago.

Cornejo, P.; Mpodozis, C.; Rivera, O.; Matthews, S.J. 2009. Carta Exploradora, Regiones de Antofagasta y Atacama. Servicio Nacional de Geología y Minería, Carta Geológica de Chile, Serie Geología Básica 119: 100 p.

Dickinson, W.R.; Gehrels, G.E. 2009. Use of U-Pb ages of zircons to infer maximum depositional ages of strata: A test against a Colorado Plateau Mesozoic database. Earth and Planetary Science Letters 288: 115-125.

García, F. 1967. Geología del Norte Grande de Chile. *In* Symposium Sobre el Geosinclinal Andino, No. 3: 138 p. Santiago.

Günther, D.; Heinrich, C.A. 1999. Enhanced sensitivity in laser ablation-ICP mass spectrometry using helium-argon mixtures as aerosol carrier. Journal of Analytical Atomic Spectrometry 14: 1363-1368.

Halpern, M. 1978. Geological significance of Rb-Sr isotopic data of northern Chile crystalline rocks of the Andean orogen between latitudes 23° and 27° South. Geological Society of America Bulletin 89: 522-532.

Hervé, F.; Faúndez, V.; Calderón, M.; Massone, H.-J.; Willner, A.P. 2007. Metamorphic and plutonic basement complexes. *In* The Geology of Chile (Moreno, T.; Gibbons, W.; editors). The Geological Society: 5-20. London.

Hoskin, P.W.O.; Schaltegger, Urs. 2003. The Composition of Zircon and Igneous and Metamorphic Petrogenesis. Reviews in Mineralogy and Geochemistry 53: 27-62.

Ludwig, K.R. 2003. User's Manual for Isoplot/Ex, Version 3.0, A Geochronological Toolkit for Microsoft Excel. Berkeley Geochronology Center Special Publication No. 4.

Maksaev, V.; Munizaga, F.; Tassinari, C. 2014. Timing of the magmatism of the paleo-Pacific border of Gondwana: U-Pb geochronology of Late Paleozoic to Early Mesozoic igneous rocks of the north Chilean Andes between 20° and 31°. Andean Geology 41 (3): 447-506. doi: 10.5027/andgeoV41n3-a01.

Morandé, J. 2014. El basamento pre-Mesozoico de la Sierra Limón Verde: Implicancias para la evolución tectónica del norte de Chile. M.Sc. Thesis (Unpublished), Departamento de Geología, Universidad de Chile: 121 p.

Niemeyer, H. 1999. Nuevos datos cinemáticos para la Falla Sierra Castillo en Quebrada del Carrizo, Precordillera de la Región de Atacama, Chile. Revista Geológica de Chile 26 (2): 159-174. doi: 10.5027/andgeoV26n2-a02.

Paton, C.; Hellstrom, J.C.; Paul, B.; Woodhead, J.D.; Hergt, J.M. 2011. Iolite: Freeware for the visualisation and processing of mass spectrometric data. Journal of Analytical Atomic Spectrometry 26: 2508-2518.

Perelló, J.; Müller, M.G. 1984. El horst de Sierra Castillo en la Cordillera de Domeyko, al occidente del Salar de Pedernales: sus fallas límites Barracas y Sierra Castillo. Universidad de Chile, Departamento. de Geología, Comunicaciones 34: 47-55. Santiago.

Pérez, E. 1982. Bioestratigrafía del Jurásico de Quebrada Asientos, Norte de Potrerillos, Región de Atacama. Servicio Nacional de Geología y Minería, Boletín 37: 149 p. Santiago.

Salazar, E.; Coloma, F.; Creixell, C. 2013. Geología del área El Tránsito-Lagunillas, Región de Atacama. Servicio Nacional de Geología y Minería, Carta Geológica de Chile, Serie Geología Básica 149: 106 p.

Slama, J.; Kosler, J.; Condon, D.J. 2008. Plesovice zircon-A new natural reference material for U-Pb and Hf isotopic microanalysis: Chemical Geology 249: 1-35.

Soto, M.F. 2013. Pressure-temperature-time paths of the Limón Verde Metamorphic Complex, Chile. M.Sc. Thesis (Unpublished), Universidad de Chile, Departamento de Geología: 125 p.

Stacey, J.S.; Kramers, J.D. 1975. Approximation of terrestrial lead isotope evolution by a two-stage model. Earth and Planetary Science Letters 26: 207-221.

Tomlinson, A.J.; Mpodozis, C.; Cornejo, P.; Ramírez, C. 1993. Structural Geology of the Sierra Castillo-Agua Amarga Fault System, Precordillera of Chile, El Salvador-Potrerillos. *In* Symposium International Géodynamique Andine, No. 2: 259-262. Oxford, Angleterre.

Tomlinson, A.J.; Cornejo, P.; Mpodozis, C. 1999. Hoja Potrerillos, Región de Atacama. Servicio Nacional de Geología y Minería, Mapas Geológicos 14: 33 p.

Tomlinson, A.J.; Blanco, N. 2008. Geología de la Franja El Abra-Chuquicamata, II Región (21°45'-22°30'S). Servicio Nacional de Geología y Minería, Informe Registrado IR-08-35: 196 p. Santiago.

Tomlinson, A.J.; Blanco, N.; García, M.; Baeza, L.; Alcota, H.; Ladino, M.; Pérez de Arce, C.; Fanning, M.; Martin, M.W. 2012. Permian exhumation of metamorphic complexes in the Calama area: Evidence for flat-slab subduction in northern Chile during the San Rafael tectonic phase and origin of the Central Andean Gravity High. *In* Congreso Geológico Chileno, No. 13, Sesión Temática 2, Geodinámica y deformación cortical Andina: 209-211, CD-ROM, Antofagasta.

Willner, A.P.; Gerdes, A.; Massonne, H.-J. 2008. History of crustal growth and recycling at the Pacific convergent margin of South America at latitudes 29°-36°S revealed by a U-Pb and Lu-Hf isotope study of detrital zircon from late Paleozoic accretionary systems. Chemical Geology 253: 114-129.

Manuscript received: December 12, 2014; revised/accepted: July 10, 2015; available online: July 13, 2015.

APPENDIX 1a. DETRITAL ZIRCON U-PB ANALYTICAL DATA OF MICA SCHISTS.

SAMPLE CHY-19; 26°23'22.05"S/69°29'09.62"W, h. 2134 m

Grain-Spot	U ppm	Th ppm	U/Th	Isotope ratios						Error Corr.	Apparent ages (Ma)						Con. %
				$^{207}Pb^*/^{206}Pb^*$	±1σ	$^{207}Pb^*/^{235}U^*$	±1σ	$^{206}Pb^*/^{238}U$	±1σ		$^{207}Pb^*/^{235}U$	±1σ	$^{207}Pb^*/^{206}Pb^*$	±1σ	$^{206}Pb^*/^{238}U^*$	±1σ	
CHY-19-1	582.0	56.4	10.2	0.0499	0.0033	0.3800	0.0250	0.0539	0.0017	0.9	326.0	20.0	200.0	130.0	338.2	10.0	169
CHY-19-2	681.0	194.0	3.5	0.0596	0.0016	0.8225	0.0360	0.0997	0.0025	1.0	609.4	21.0	590.3	61.0	612.5	15.0	104
CHY-19-3	1,166.0	202.0	6.3	0.0532	0.0015	0.3866	0.0170	0.0526	0.0012	0.2	331.9	12.0	336.0	64.0	330.5	7.5	98
CHY-19-4	460.0	184.1	3.4	0.0598	0.0017	0.7881	0.0340	0.0958	0.0025	0.4	590.1	20.0	597.8	61.0	589.8	14.0	99
CHY-19-5	345.7	166.0	2.0	0.0586	0.0017	0.6556	0.1100	0.0818	0.0022	1.0	511.9	89.0	551.2	62.0	506.5	13.0	92
CHY-19-6	161.3	66.1	2.0	0.0753	0.0021	1.8051	0.0760	0.1746	0.0044	0.6	1,047.3	29.0	1,075.4	57.0	1,037.3	24.0	96
CHY-19-7	573.4	768.0	0.6	0.0539	0.0015	0.3749	0.0160	0.0507	0.0013	0.8	323.3	12.0	367.1	63.0	318.8	8.2	87
CHY-19-8	743.0	548.0	1.7	0.0524	0.0015	0.4121	0.0180	0.0584	0.0016	0.8	350.4	13.0	303.0	64.0	365.9	9.7	121
CHY-19-9	157.0	97.0	1.3	0.0601	0.0017	0.7610	0.0520	0.0914	0.0025	0.8	574.5	36.0	605.0	61.0	563.5	15.0	93
CHY-19-10	146.5	39.9	5.8	0.0749	0.0021	1.8010	0.0830	0.1743	0.0044	0.9	1,045.6	30.0	1,065.2	57.0	1,035.9	24.0	97
CHY-19-11	507.0	44.8	9.5	0.0535	0.0015	0.3914	0.0180	0.0535	0.0014	0.6	335.4	13.0	348.0	64.0	336.1	8.3	97
CHY-19-12	240.0	98.8	2.1	0.0579	0.0017	0.6790	0.0740	0.0863	0.0023	0.7	526.6	55.0	526.0	63.0	533.6	14.0	101
CHY-19-13	230.4	90.6	2.2	0.0603	0.0017	0.8189	0.0440	0.0998	0.0027	0.9	607.4	27.0	613.7	61.0	613.4	16.0	100
CHY-19-14	381.0	135.0	2.6	0.0558	0.0016	0.5668	0.0830	0.0746	0.0022	1.0	455.8	64.0	444.0	67.0	463.7	13.0	104
CHY-19-15	367.0	432.7	0.8	0.0741	0.0022	1.7920	0.0840	0.1768	0.0046	0.7	1,042.4	30.0	1,044.0	57.0	1,049.3	25.0	101
CHY-19-16	104.0	42.3	2.4	0.0594	0.0018	0.7240	0.0490	0.0892	0.0024	0.8	552.7	30.0	580.0	63.0	550.7	14.0	95
CHY-19-17	850.0	89.7	9.5	0.0528	0.0015	0.3877	0.0180	0.0536	0.0014	0.7	332.7	14.0	318.6	64.0	336.8	8.7	106
CHY-19-18	535.0	572.0	0.9	0.0615	0.0017	0.8190	0.0380	0.0963	0.0025	0.9	607.5	22.0	655.4	60.0	592.9	14.0	90
CHY-19-19	224.0	194.0	1.2	0.0623	0.0018	0.8712	0.0420	0.1011	0.0026	0.6	636.2	25.0	684.8	61.0	620.9	15.0	91
CHY-19-20	650.0	426.0	1.7	0.0564	0.0016	0.6965	0.0320	0.0908	0.0024	0.8	536.7	19.0	469.3	62.0	560.0	14.0	119
CHY-19-21	523.0	117.5	5.6	0.0735	0.0020	1.7610	0.0810	0.1758	0.0045	0.9	1,031.2	30.0	1,027.7	55.0	1,044.0	25.0	102
CHY-19-22	261.3	98.3	2.3	0.0599	0.0017	0.7590	0.0550	0.0915	0.0024	0.9	573.1	36.0	599.0	62.0	564.5	14.0	94
CHY-19-23	750.0	532.0	1.2	0.0533	0.0015	0.4228	0.0190	0.0575	0.0015	0.9	358.1	13.0	344.0	61.0	360.6	8.9	105
CHY-19-24	245.0	165.0	1.2	0.0573	0.0017	0.5938	0.0270	0.0759	0.0019	0.7	473.3	17.0	503.0	64.0	471.5	11.0	94
CHY-19-25	452.0	231.8	1.7	0.0573	0.0016	0.6772	0.0300	0.0863	0.0022	0.0	525.0	18.0	504.0	63.0	533.5	13.0	106
CHY-19-26	890.0	85.4	9.5	0.0524	0.0015	0.3876	0.0180	0.0543	0.0014	0.8	332.6	13.0	302.1	64.0	341.0	8.7	113
CHY-19-27	325.0	126.5	2.7	0.0705	0.0020	1.4179	0.0630	0.1449	0.0037	0.7	897.3	27.0	942.9	58.0	872.3	21.0	93
CHY-19-28	595.0	562.0	1.0	0.0605	0.0019	0.8690	0.0460	0.1046	0.0031	1.0	634.9	27.0	622.0	68.0	641.2	18.0	103
CHY-19-29	730.0	121.0	8.4	0.0590	0.0014	0.7200	0.0370	0.0887	0.0038	1.0	550.0	24.0	565.0	60.0	548.0	22.0	97
CHY-19-30	527.0	227.2	2.1	0.0594	0.0013	0.7024	0.0700	0.0861	0.0024	0.8	540.2	54.0	580.0	67.0	532.5	14.0	92
CHY-19-31	317.0	209.0	1.4	0.0599	0.0013	0.7008	0.0480	0.0849	0.0022	0.7	539.2	37.0	598.0	59.0	525.0	13.0	88
CHY-19-32	383.0	71.3	4.9	0.0589	0.0009	0.7627	0.0900	0.0956	0.0100	0.8	575.6	52.0	561.4	32.0	588.0	60.0	105
~~CHY-19-33~~	~~95.0~~	~~7.3~~	~~13.0~~	~~0.0330~~	~~0.0130~~	~~0.4000~~	~~0.1600~~	~~0.0873~~	~~0.0094~~	~~0.5~~	~~310.0~~	~~140.0~~	~~-480.0~~	~~510.0~~	~~539.0~~	~~55.0~~	
CHY-19-34	540.0	1530.0	0.3	0.0540	0.0009	0.5820	0.0710	0.0766	0.0084	1.0	466.0	46.0	369.0	36.0	476.0	50.0	129

Appendix 1a. continued.

Grain-Spot	U ppm	Th ppm	U/Th	Isotope ratios						Error Corr.	Apparent ages (Ma)						Con. %
				$^{207}Pb^*/^{206}Pb^*$	±1σ	$^{207}Pb^*/^{235}U^*$	±1σ	$^{206}Pb^*/^{238}U$	±1σ		$^{207}Pb^*/^{235}U$	±1σ	$^{207}Pb^*/^{206}Pb^*$	±1σ	$^{206}Pb^*/^{238}U^*$	±1σ	
CHY-19-35	849.0	352.1	2.4	0.0555	0.0012	0.4170	0.0510	0.0532	0.0056	0.9	354.0	36.0	432.0	48.0	334.4	34.0	77
CHY-19-36	534.0	211.2	2.5	0.0589	0.0009	0.8488	0.1000	0.1023	0.0110	1.0	624.0	55.0	563.9	32.0	628.0	63.0	111
CHY-19-37	444.0	174.4	2.5	0.0590	0.0009	0.7867	0.0930	0.0937	0.0097	0.9	589.3	53.0	568.4	32.0	577.5	57.0	102
CHY-19-38	690.0	460.0	1.5	0.0567	0.0009	0.5970	0.0810	0.0745	0.0091	1.0	475.0	52.0	478.0	35.0	463.0	55.0	97
CHY-19-39	507.0	54.8	9.3	0.0568	0.0008	0.6453	0.0760	0.0816	0.0085	0.9	505.5	47.0	484.2	32.0	505.6	51.0	104
CHY-19-40	859.0	1,024.0	0.8	0.0532	0.0008	0.3887	0.0460	0.0518	0.0054	1.0	333.4	34.0	338.0	33.0	325.7	33.0	96
CHY-19-41	220.0	137.8	1.6	0.0614	0.0009	0.9184	0.1100	0.1066	0.0110	1.0	661.5	57.0	651.4	31.0	653.2	65.0	100
CHY-19-42	577.0	498.0	1.2	0.0538	0.0008	0.4550	0.0530	0.0628	0.0065	0.3	380.8	37.0	363.1	33.0	392.8	40.0	108
CHY-19-43	481.0	65.3	7.4	0.0585	0.0008	0.6953	0.0820	0.0848	0.0088	1.0	536.0	49.0	546.6	32.0	524.8	52.0	96
CHY-19-44	382.0	44.9	8.8	0.0587	0.0009	0.6971	0.0820	0.0851	0.0089	0.9	537.0	49.0	554.5	32.0	526.3	53.0	95
CHY-19-45	553.0	1,193.0	0.5	0.0552	0.0009	0.4930	0.0590	0.0645	0.0068	0.9	406.7	40.0	419.0	36.0	402.7	41.0	96
CHY-19-46	217.0	172.0	1.3	0.0611	0.0009	0.8976	0.1100	0.1060	0.0110	0.9	650.4	57.0	641.1	31.0	649.5	64.0	101
CHY-19-47	559.0	326.0	1.9	0.0544	0.0008	0.4550	0.0540	0.0608	0.0064	0.9	380.8	37.0	385.3	34.0	380.7	39.0	99
CHY-19-48	218.0	147.2	1.5	0.0654	0.0010	1.1970	0.1400	0.1323	0.0140	0.8	799.1	65.0	785.4	31.0	801.0	79.0	102
CHY-19-49	270.0	169.0	1.7	0.0611	0.0009	0.8610	0.1000	0.1032	0.0110	0.9	630.5	55.0	643.5	31.0	633.1	63.0	98
CHY-19-50	170.0	233.0	0.8	0.0604	0.0009	0.8500	0.1000	0.1038	0.0110	1.0	624.4	55.0	616.8	31.0	636.0	64.0	103
CHY-19-51	325.0	104.0	3.3	0.0581	0.0009	0.7030	0.0840	0.0893	0.0094	0.6	540.0	51.0	534.3	32.0	552.0	56.0	103
CHY-19-52	383.0	169.8	2.5	0.0582	0.0008	0.6777	0.0800	0.0859	0.0090	1.0	525.3	48.0	537.3	32.0	531.5	53.0	99
CHY-19-53	462.0	66.2	7.9	0.0606	0.0010	0.7490	0.0930	0.0905	0.0100	0.8	570.0	57.0	623.0	35.0	558.0	59.0	90
CHY-19-54	160.0	76.0	2.2	0.0624	0.0009	0.9900	0.1200	0.1176	0.0120	0.9	698.5	60.0	688.2	31.0	716.0	71.0	104
CHY-19-55	107.8	251.0	0.5	0.0572	0.0008	0.7377	0.0870	0.0966	0.0100	0.9	561.0	51.0	498.9	32.0	594.3	60.0	119
CHY-19-56	468.0	126.0	4.0	0.0583	0.0008	0.6920	0.0820	0.0870	0.0092	0.9	533.7	49.0	539.9	31.0	537.9	54.0	100
CHY-19-57	226.0	122.1	2.0	0.0581	0.0008	0.6763	0.0800	0.0854	0.0089	1.0	524.5	48.0	533.3	32.0	528.3	53.0	99
CHY-19-58	174.0	95.3	2.0	0.0583	0.0008	0.6677	0.0790	0.0845	0.0089	0.9	519.3	48.0	542.4	32.0	522.7	53.0	96
CHY-19-59	158.0	79.2	2.2	0.0595	0.0009	0.7489	0.0880	0.0931	0.0097	0.9	567.6	51.0	587.1	31.0	574.0	57.0	98
CHY-19-60	206.0	134.0	1.7	0.0595	0.0009	0.7420	0.0870	0.0921	0.0096	0.9	563.6	51.0	585.5	31.0	568.0	56.0	97
CHY-19-61	183.0	105.3	1.9	0.0766	0.0011	1.9130	0.2200	0.1845	0.0190	0.5	1,085.5	78.0	1,111.8	29.0	1,091.7	100.0	98
CHY-19-62	95.0	29.9	3.5	0.0593	0.0009	0.6912	0.0810	0.0866	0.0090	1.0	533.5	49.0	579.2	32.0	535.6	53.0	92
CHY-19-63	125.0	86.6	1.6	0.0597	0.0009	0.7443	0.0870	0.0927	0.0096	0.7	564.9	51.0	593.0	31.0	571.6	57.0	96
CHY-19-64	201.9	150.5	1.5	0.0574	0.0008	0.5726	0.0680	0.0741	0.0077	0.9	459.7	44.0	507.9	32.0	460.9	46.0	91
CHY-19-65	145.0	105.4	1.5	0.0603	0.0009	0.7469	0.0880	0.0924	0.0096	0.9	566.3	51.0	615.3	32.0	569.6	57.0	93
CHY-19-66	152.0	101.7	1.8	0.0600	0.0009	0.7397	0.0870	0.0922	0.0096	0.9	562.2	51.0	602.2	31.0	568.5	57.0	94
~~CHY-19-67~~	~~13.0~~	~~3.3~~	~~4.7~~	~~0.0170~~	~~0.0220~~	~~0.2000~~	~~0.2600~~	~~0.0869~~	~~0.0092~~	~~0.7~~	~~140.0~~	~~240.0~~	~~1,090.0~~	~~870.0~~	~~537.0~~	~~54.0~~	-
CHY-19-68	120.0	37.5	3.5	0.0754	0.0011	1.7190	0.2000	0.1731	0.0180	0.8	1015.0	76.0	1,078.5	30.0	1,029.0	100.0	95
CHY-19-69	143.0	80.9	2.0	0.0739	0.0011	1.6060	0.1900	0.1690	0.0180	0.9	972.0	76.0	1,038.6	29.0	1,006.0	99.0	97
CHY-19-70	114.7	156.2	0.8	0.0620	0.0009	0.8585	0.1000	0.1032	0.0110	0.9	629.3	55.0	674.4	31.0	633.2	63.0	94
CHY-19-71	337.0	68.6	5.5	0.0605	0.0009	0.7134	0.0840	0.0879	0.0092	1.0	546.7	50.0	621.7	32.0	542.9	54.0	87

Appendix 1a. continued.

SAMPLE CHY-79; 25°55'25.37"S/69°20'13.91"W, h. 2866 m

Grain-Spot	U ppm	Th ppm	U/Th	Isotope ratios						Error Corr.	Apparent ages (Ma)						Con. %
				$^{207}Pb^*/^{206}Pb^*$	±1σ	$^{207}Pb^*/^{235}U^*$	±1σ	$^{206}Pb^*/^{238}U$	±1σ		$^{207}Pb^*/^{235}U$	±1σ	$^{207}Pb^*/^{206}Pb^*$	±1σ	$^{206}Pb^*/^{238}U^*$	±1σ	
~~CHY-79-1~~	~~157.0~~	~~86.0~~	~~1.7~~	~~0.0448~~	~~0.0073~~	~~0.4240~~	~~0.0720~~	~~0.0690~~	~~0.0015~~	~~0.3~~	~~356.0~~	~~54.0~~	~~-10.0~~	~~300.0~~	~~430.3~~	~~9.0~~	-
CHY-79-2	441.0	42.6	9.9	0.0606	0.0042	0.6650	0.0630	0.0781	0.0033	0.9	517.0	38.0	624.0	150.0	485.0	20.0	78
CHY-79-3	455.0	177.0	2.2	0.0528	0.0035	0.3649	0.0310	0.0503	0.0008	0.9	315.8	23.0	320.3	150.0	316.5	4.9	99
CHY-79-4	346.0	102.0	2.9	0.0527	0.0035	0.3545	0.0310	0.0491	0.0009	0.9	308.1	23.0	317.0	150.0	309.2	5.7	98
CHY-79-5	890.0	337.0	2.1	0.0592	0.0039	0.6060	0.0530	0.0745	0.0019	0.8	480.8	34.0	574.0	150.0	463.2	11.0	81
CHY-79-6	298.0	114.8	2.0	0.0542	0.0037	0.3609	0.0310	0.0491	0.0009	0.7	312.9	23.0	380.0	150.0	308.8	5.7	81
CHY-79-7	603.0	181.0	2.6	0.0635	0.0043	0.6800	0.0620	0.0788	0.0038	1.0	526.0	37.0	724.0	140.0	489.0	23.0	68
CHY-79-8	415.0	131.0	2.3	0.0775	0.0051	1.7920	0.1600	0.1701	0.0055	1.0	1,042.0	60.0	1,133.0	130.0	1,013.0	30.0	89
CHY-79-9	108.3	64.1	1.3	0.0923	0.0061	2.1840	0.1900	0.1740	0.0040	1.0	1,176.0	61.0	1,472.9	130.0	1,034.0	22.0	70
CHY-79-10	620.0	208.0	2.5	0.0557	0.0037	0.3241	0.0280	0.0428	0.0008	1.0	285.0	21.0	441.1	150.0	270.0	5.1	61
CHY-79-11	756.0	340.0	1.9	0.0569	0.0038	0.3274	0.0280	0.0422	0.0007	0.1	287.6	21.0	486.0	150.0	266.5	4.2	55
CHY-79-12	673.0	284.0	2.4	0.0558	0.0037	0.3414	0.0290	0.0449	0.0007	0.9	298.2	22.0	442.0	150.0	283.1	4.4	64
CHY-79-13	389.0	256.7	1.5	0.0600	0.0040	0.7420	0.0650	0.0908	0.0024	1.0	563.4	37.0	604.7	140.0	560.0	14.0	93
CHY-79-14	610.0	280.0	2.2	0.0586	0.0049	0.3650	0.0360	0.0458	0.0011	0.9	316.0	27.0	540.0	170.0	288.8	7.0	53
CHY-79-15	497.0	235.8	2.0	0.0569	0.0038	0.5580	0.0500	0.0728	0.0019	1.0	454.5	21.0	488.0	150.0	452.8	11.0	93
CHY-79-16	450.4	328.0	1.2	0.0545	0.0036	0.3499	0.0300	0.0467	0.0010	0.9	304.6	23.0	391.0	150.0	294.5	6.0	75
CHY-79-17	220.3	149.1	1.3	0.0569	0.0038	0.5845	0.0500	0.0749	0.0015	0.5	467.3	32.0	487.0	150.0	465.3	8.8	96
CHY-79-18	337.0	203.0	1.3	0.0570	0.0039	0.3416	0.0310	0.0438	0.0010	0.8	298.3	23.0	491.0	150.0	276.5	6.2	56
CHY-79-19	491.0	368.0	1.1	0.0638	0.0046	0.7420	0.0660	0.0851	0.0014	0.4	563.0	38.0	730.0	160.0	526.5	8.3	72
CHY-79-20	870.0	30.9	20.9	0.0578	0.0040	0.5790	0.0530	0.0725	0.0020	0.9	464.0	34.0	523.0	150.0	451.0	12.0	86
CHY-79-21	613.0	169.0	2.7	0.0606	0.0040	0.6300	0.0580	0.0759	0.0029	1.0	496.0	36.0	624.0	140.0	472.0	17.0	76
CHY-79-22	513.0	189.0	2.1	0.0638	0.0042	0.9089	0.0770	0.1042	0.0017	0.9	656.5	41.0	733.9	140.0	638.7	9.7	87
CHY-79-23	662.0	291.0	1.8	0.0666	0.0051	0.3324	0.0290	0.0365	0.0015	0.1	291.4	22.0	817.0	160.0	231.1	9.1	28
CHY-79-24	1,040.0	394.0	2.3	0.0534	0.0035	0.3653	0.0310	0.0497	0.0010	1.0	316.1	23.0	344.0	150.0	312.6	6.1	91
CHY-79-25	529.0	177.2	2.7	0.0755	0.0050	1.4660	0.1300	0.1394	0.0021	1.0	916.0	52.0	1,080.6	130.0	841.1	12.0	78
CHY-79-26	1,207.0	459.0	2.4	0.0587	0.0040	0.2992	0.0270	0.0371	0.0012	1.0	265.7	21.0	556.0	150.0	234.7	7.6	42
CHY-79-27	417.0	189.9	2.1	0.0787	0.0052	2.0100	0.1700	0.1853	0.0030	0.9	1,118.7	58.0	1,163.2	130.0	1,096.0	16.0	94
CHY-79-28	1,728.0	1542.0	1.1	0.0606	0.0040	0.4060	0.0350	0.0485	0.0013	1.0	346.0	25.0	625.0	140.0	305.4	7.7	49
CHY-79-29	366.0	127.3	3.2	0.0758	0.0051	1.3940	0.1200	0.1332	0.0030	1.0	886.0	52.0	1,089.0	130.0	806.0	17.0	74
CHY-79-30	1,885.0	480.0	4.5	0.0548	0.0037	0.3453	0.0300	0.0455	0.0007	0.5	301.2	23.0	403.0	150.0	287.0	4.4	71

Appendix 1a. continued.

Grain-Spot	U ppm	Th ppm	U/Th	Isotope ratios						Error Corr.	Apparent ages (Ma)						Con. %
				$^{207}Pb^*/^{206}Pb^*$	±1σ	$^{207}Pb^*/^{235}U^*$	±1σ	$^{206}Pb^*/^{238}U$	±1σ		$^{207}Pb^*/^{235}U$	±1σ	$^{207}Pb^*/^{206}Pb^*$	±1σ	$^{206}Pb^*/^{238}U^*$	±1σ	
CHY-79-31	227.0	255.0	1.0	0.0780	0.0052	1.9540	0.1700	0.1806	0.0030	1.0	1,099.9	57.0	1,146.4	130.0	1,070.2	16.0	93
CHY-79-32	428.0	210.0	2.4	0.0599	0.0040	0.6430	0.0560	0.0774	0.0018	1.0	504.3	34.0	598.8	140.0	480.8	11.0	80
CHY-79-33	516.8	357.8	1.6	0.0608	0.0040	0.5150	0.0440	0.0613	0.0011	0.9	421.8	29.0	630.0	140.0	383.5	6.7	61
CHY-79-34	559.0	429.0	1.4	0.0567	0.0038	0.5670	0.0480	0.0720	0.0011	0.9	456.0	31.0	480.5	150.0	448.0	6.7	93
CHY-79-35	198.0	122.0	1.5	0.0622	0.0044	0.3749	0.0320	0.0440	0.0011	0.5	323.2	24.0	679.0	150.0	277.3	7.0	41
CHY-79-36	309.0	170.0	1.7	0.0601	0.0040	0.3480	0.0300	0.0423	0.0009	0.9	303.2	22.0	607.0	150.0	266.8	5.6	44
CHY-79-37	350.0	263.0	1.2	0.0633	0.0043	0.5860	0.0510	0.0664	0.0012	0.4	468.0	32.0	716.0	140.0	414.5	7.5	58
CHY-79-38	425.0	198.0	1.9	0.0629	0.0042	0.3185	0.0280	0.0366	0.0010	0.8	280.7	21.0	704.0	140.0	231.5	6.1	33
CHY-79-39	784.6	264.9	2.7	0.0538	0.0036	0.3527	0.0300	0.0475	0.0007	0.7	306.7	23.0	362.0	150.0	299.4	4.6	83
CHY-79-40	234.6	102.1	2.1	0.0745	0.0049	1.7516	0.1500	0.1704	0.0026	0.7	1,027.7	55.0	1,055.6	130.0	1,014.2	14.0	96
CHY-79-41	498.0	233.0	2.1	0.0632	0.0042	0.9333	0.0800	0.1073	0.0017	0.9	669.4	42.0	714.7	140.0	656.9	10.0	92
CHY-79-42	482.0	145.0	3.2	0.0567	0.0039	0.3353	0.0290	0.0430	0.0015	0.9	293.6	22.0	478.0	150.0	271.5	9.1	57
CHY-79-43	703.6	336.0	2.1	0.0761	0.0051	1.3660	0.1200	0.1304	0.0033	0.9	874.0	52.0	1,098.0	130.0	790.0	19.0	72
CHY-79-44	339.0	260.0	1.3	0.0526	0.0035	0.3219	0.0280	0.0446	0.0009	0.9	283.3	21.0	311.0	150.0	281.0	5.6	90
CHY-79-45	910.0	580.0	1.5	0.0634	0.0044	0.7250	0.0690	0.0833	0.0040	0.8	553.0	41.0	719.0	140.0	515.0	24.0	72
CHY-79-46	751.0	284.0	2.4	0.0573	0.0041	0.3450	0.0340	0.0440	0.0011	0.7	301.0	26.0	499.0	160.0	277.3	6.6	56
CHY-79-47	404.0	541.0	0.7	0.0597	0.0039	0.7030	0.0600	0.0857	0.0016	1.0	540.5	36.0	591.0	140.0	529.8	9.7	90
CHY-79-48	780.0	526.0	1.3	0.0587	0.0041	0.3510	0.0360	0.0432	0.0023	1.0	305.0	27.0	555.0	150.0	272.0	14.0	49
CHY-79-49	386.0	80.4	4.0	0.0666	0.0044	1.0200	0.0900	0.1112	0.0030	1.0	714.0	45.0	826.0	140.0	680.0	18.0	82
CHY-79-50	651.0	68.4	7.6	0.0573	0.0038	0.6146	0.0530	0.0780	0.0016	1.0	486.4	33.0	503.0	150.0	484.1	9.8	96
CHY-79-51	331.7	152.9	1.7	0.0729	0.0048	1.3770	0.1200	0.1374	0.0030	1.0	879.2	51.0	1,011.8	130.0	830.0	17.0	82
CHY-79-52	875.0	230.0	2.9	0.0533	0.0035	0.3154	0.0270	0.0430	0.0008	1.0	278.3	21.0	341.8	150.0	271.4	4.7	79
CHY-79-53	463.0	121.5	3.0	0.0617	0.0041	0.8490	0.0730	0.1003	0.0019	1.0	624.2	40.0	662.2	140.0	615.9	11.0	93
CHY-79-54	455.0	213.2	1.6	0.0601	0.0042	0.6480	0.0580	0.0785	0.0016	0.6	507.0	36.0	604.0	150.0	486.9	9.8	81
CHY-79-55	415.4	188.6	1.7	0.0579	0.0039	0.5174	0.0440	0.0649	0.0010	0.7	423.4	30.0	527.0	150.0	405.5	6.1	77
CHY-79-56	350.0	186.0	1.4	0.0587	0.0039	0.6590	0.0570	0.0819	0.0018	1.0	513.9	35.0	554.0	140.0	507.3	10.0	92
CHY-79-57	476.0	357.6	1.1	0.0543	0.0036	0.3548	0.0300	0.0480	0.0008	0.8	308.3	23.0	382.8	150.0	302.1	4.9	79
CHY-79-58	1570.0	201.0	6.3	0.0610	0.0043	0.4890	0.0450	0.0576	0.0023	0.9	404.0	31.0	638.0	150.0	361.0	14.0	57
CHY-79-59	247.0	209.0	0.9	0.0809	0.0054	2.1390	0.1800	0.1932	0.0034	0.6	1,161.5	59.0	1,218.4	130.0	1,138.7	18.0	93
CHY-79-60	944.0	148.0	5.2	0.0575	0.0038	0.5496	0.0470	0.0699	0.0012	1.0	444.7	31.0	509.2	150.0	435.5	7.3	86
CHY-79-61	692.0	400.0	1.4	0.0624	0.0042	0.2761	0.0240	0.0324	0.0007	0.8	247.6	19.0	688.0	140.0	205.5	4.1	30

Appendix 1a. continued.

SAMPLE CHY-80; 25°55'25.37"S/69°20'13.91"W, h. 2866 m

Grain-Spot	U ppm	Th ppm	U/Th	Isotope ratios						Error Corr.	Apparent ages (Ma)						Con. %
				$^{207}Pb^*/^{206}Pb^*$	±1σ	$^{207}Pb^*/^{235}U^*$	±1σ	$^{206}Pb^*/^{238}U$	±1σ		$^{207}Pb^*/^{235}U$	±1σ	$^{207}Pb^*/^{206}Pb^*$	±1σ	$^{206}Pb^*/^{238}U^*$	±1σ	
CHY-80-1	558.0	141.3	4.5	0.05361	0.00320	0.37090	0.02600	0.04988	0.00120	0.7	320.3	19.0	355.0	140	313.8	7.3	88
CHY-80-2	477.9	204.8	2.6	0.07829	0.00460	1.97550	0.14000	0.18253	0.00430	0.8	1,107.2	46.0	1,154.3	120	1,080.8	24.0	94
CHY-80-3	386.1	354.0	1.2	0.08143	0.00480	2.23500	0.15000	0.19910	0.00490	0.9	1,192.2	48.0	1,231.8	120	1,170.3	27.0	95
CHY-80-4	409.0	338.0	1.3	0.08217	0.00490	1.45500	0.10000	0.16813	0.00400	0.9	918.0	77.0	1,249.6	120	1,001.8	22.0	80
CHY-80-5	752.0	543.0	1.4	0.05455	0.00320	0.34110	0.02400	0.04561	0.00130	1.0	297.9	19.0	393.0	130	287.5	8.1	73
CHY-80-6	2,040.0	874.0	2.2	0.05588	0.00340	0.36060	0.02600	0.04800	0.00160	0.9	312.6	20.0	447.0	130	302.1	9.9	68
CHY-80-7	1,154.2	60.1	18.3	0.07012	0.00420	1.25650	0.08800	0.13155	0.00320	0.9	826.3	40.0	931.9	120	796.7	18.0	85
~~CHY-80-8~~	~~74.0~~	~~4.7~~	~~16.6~~	~~0.06420~~	~~0.00400~~	~~1.55000~~	~~0.27000~~	~~0.18400~~	~~0.02900~~	~~1.0~~	~~941.0~~	~~110.0~~	~~748.0~~	~~130~~	~~1,090.0~~	~~160.0~~	-
CHY-80-9	279.0	94.5	3.0	0.06217	0.00380	0.69400	0.05000	0.08090	0.00250	0.7	535.2	30.0	679.0	120	501.4	15.0	74
CHY-80-10	895.0	63.7	13.5	0.05892	0.00350	0.57600	0.04100	0.07180	0.00220	1.0	461.8	26.0	564.3	130	446.9	13.0	79
CHY-80-11	1,098.0	622.0	1.7	0.05437	0.00330	0.33320	0.02400	0.04450	0.00160	1.0	291.9	18.0	392.0	110	280.6	9.8	72
CHY-80-12	819.0	94.0	7.8	0.07070	0.00470	0.94000	0.13000	0.09680	0.00990	1.0	672.0	67.0	948.0	130	595.0	58.0	63
CHY-80-13	196.0	157.0	1.2	0.12370	0.00750	5.14000	0.50000	0.30400	0.02000	1.0	1,837.0	87.0	2,009.0	110	1,707.0	100.0	85
CHY-80-14	830.0	536.0	1.7	0.05828	0.00350	0.33400	0.02700	0.04070	0.00170	1.0	293.0	21.0	540.0	130	256.9	11.0	48
CHY-80-15	500.0	172.5	3.1	0.06958	0.00410	0.89300	0.07000	0.09280	0.00400	1.0	647.0	37.0	915.8	120	572.0	24.0	62
CHY-80-16	511.0	63.9	8.4	0.05717	0.00340	0.59220	0.04200	0.07510	0.00200	1.0	472.2	27.0	498.2	130	466.8	12.0	94
CHY-80-17	952.0	197.0	7.4	0.05719	0.00340	0.60470	0.04200	0.07670	0.00200	1.0	480.2	27.0	498.8	130	476.4	12.0	96
CHY-80-18	179.0	120.6	1.5	0.05294	0.00320	0.32270	0.02300	0.04430	0.00110	0.2	284.0	17.0	326.0	140	279.4	6.8	86
CHY-80-19	267.0	87.0	2.7	0.07499	0.00450	1.81600	0.14000	0.17620	0.00680	1.0	1,051.0	50.0	1,068.3	120	1,046.0	38.0	98
CHY-80-20	147.2	97.1	1.3	0.12854	0.00760	6.57000	0.47000	0.37220	0.01200	1.0	2,055.0	63.0	2,078.1	100	2,040.0	54.0	98
CHY-80-21	30.0	19.9	1.4	0.12030	0.00830	5.87000	0.50000	0.35490	0.00910	0.5	1,954.0	73.0	1,956.0	130	1,958.0	43.0	100
CHY-80-22	360.0	166.0	2.0	0.05366	0.00320	0.34950	0.02500	0.04755	0.00120	0.9	304.3	19.0	356.0	130	299.4	7.3	84
CHY-80-23	1,239.0	386.4	3.0	0.05319	0.00320	0.37400	0.02600	0.05131	0.00120	1.0	322.6	19.0	336.8	140	322.5	7.6	96
CHY-80-24	460.0	266.0	1.8	0.06280	0.00410	0.35900	0.03400	0.04150	0.00190	0.9	311.0	25.0	700.0	140	262.0	12.0	37
CHY-80-25	180.9	149.0	1.3	0.05229	0.00310	0.32840	0.02300	0.04567	0.00110	0.7	288.3	18.0	298.0	140	287.9	6.8	97
CHY-80-26	81.0	78.5	1.0	0.08147	0.00490	2.31900	0.16000	0.20500	0.00530	0.9	1,218.0	49.0	1,233.0	120	1,202.0	28.0	97
CHY-80-27	460.0	167.0	3.4	0.05790	0.00690	0.64000	0.12000	0.08820	0.00640	0.3	519.0	60.0	510.0	280	545.0	38.0	107
CHY-80-28	540.0	178.0	3.0	0.06130	0.00380	0.89500	0.06900	0.10230	0.00340	1.0	649.0	37.0	649.0	140	628.0	20.0	97
CHY-80-29	449.0	393.0	1.1	0.06390	0.00540	0.39900	0.03700	0.04358	0.00110	0.5	340.0	27.0	700.0	180	275.0	6.5	39
CHY-80-30	521.9	391.4	1.3	0.05286	0.00290	0.35200	0.02400	0.04672	0.00110	0.8	306.2	18.0	322.6	120	294.4	6.8	91
CHY-80-31	237.0	436.0	0.6	0.06240	0.00370	0.89100	0.06300	0.10070	0.00260	1.0	646.8	34.0	687.9	130	618.7	15.0	90
CHY-80-32	853.0	265.0	3.4	0.05830	0.00370	0.36680	0.02700	0.04400	0.00190	1.0	317.2	20.0	537.0	140	277.5	12.0	52
CHY-80-33	1,146.0	532.0	2.2	0.05388	0.00320	0.35430	0.02500	0.04601	0.00130	1.0	307.9	19.0	366.0	130	290.0	7.7	79
CHY-80-34	850.0	268.0	3.2	0.05427	0.00330	0.37210	0.02700	0.04770	0.00170	1.0	321.1	20.0	394.0	130	300.2	10.0	76

Appendix 1a. continued.

Grain-Spot	U ppm	Th ppm	U/Th	Isotope ratios						Error Corr.	Apparent ages (Ma)						Con. %
				$^{207}Pb^*/^{206}Pb^*$	±1σ	$^{207}Pb^*/^{235}U^*$	±1σ	$^{206}Pb^*/^{238}U$	±1σ		$^{207}Pb^*/^{235}U$	±1σ	$^{207}Pb^*/^{206}Pb^*$	±1σ	$^{206}Pb^*/^{238}U^*$	±1σ	
CHY-80-35	1,271.0	216.0	6.5	0.06660	0.00410	0.45400	0.04800	0.04710	0.00310	1.0	379.0	33.0	824.0	130	297.0	19.0	36
CHY-80-36	832.0	641.0	1.5	0.06066	0.00360	0.75730	0.05300	0.08801	0.00210	0.8	572.4	31.0	627.2	130	543.8	13.0	87
CHY-80-37	2,174.0	1,184.0	2.1	0.05413	0.00320	0.32870	0.02300	0.04256	0.00120	1.0	288.6	18.0	376.2	130	268.7	7.5	71
CHY-80-38	570.0	505.0	1.3	0.05389	0.00320	0.35780	0.02500	0.04629	0.00120	0.9	310.6	19.0	366.4	130	291.7	7.1	80
CHY-80-39	643.0	198.0	3.6	0.06069	0.00360	0.73500	0.05200	0.08439	0.00220	0.9	559.5	30.0	628.3	130	522.3	13.0	83
CHY-80-40	640.0	103.0	6.8	0.05522	0.00340	0.40700	0.04200	0.05110	0.00380	1.0	346.0	32.0	420.0	140	321.0	23.0	76
CHY-80-41	625.0	69.9	9.2	0.05701	0.00340	0.59740	0.04200	0.07350	0.00200	1.0	475.6	27.0	491.9	130	457.0	12.0	93
CHY-80-42	647.0	67.0	10.0	0.05700	0.00340	0.60230	0.04200	0.07383	0.00180	0.9	478.7	27.0	491.5	130	459.2	11.0	93
CHY-80-43	384.0	286.0	1.3	0.05523	0.00330	0.46250	0.03200	0.05796	0.00140	0.5	386.0	22.0	421.0	130	363.2	8.7	86
CHY-80-44	182.5	54.1	3.4	0.05835	0.00350	0.67590	0.04700	0.08013	0.00190	0.4	524.3	28.0	542.7	130	496.9	11.0	92
CHY-80-45	290.9	82.9	3.5	0.05809	0.00350	0.65510	0.04500	0.07818	0.00180	1.0	514.0	75.0	533.0	130	485.3	11.0	91
CHY-80-46	250.0	44.9	5.6	0.07257	0.00430	1.72000	0.12000	0.16460	0.00490	1.0	1,016.0	45.0	1,002.1	120	982.0	27.0	98
CHY-80-47	319.0	37.3	9.1	0.07259	0.00430	1.68900	0.12000	0.16150	0.00400	1.0	1,004.3	45.0	1,002.6	120	965.2	22.0	96
CHY-80-48	670.0	28.2	23.5	0.05948	0.00360	0.67500	0.05300	0.07950	0.00360	0.9	524.0	32.0	585.0	130	493.0	22.0	84
CHY-80-49	370.0	104.2	3.2	0.07622	0.00450	1.83600	0.15000	0.16880	0.00810	1.0	1,057.0	54.0	1,100.7	120	1,005.0	45.0	91
~~CHY-80-50~~	~~1,310.0~~	~~307.7~~	~~3.4~~	~~0.05978~~	~~0.00360~~	~~0.29100~~	~~0.02300~~	~~0.03440~~	~~0.00180~~	~~1.0~~	~~259.0~~	~~18.0~~	~~595.0~~	~~130~~	~~218.0~~	~~11.0~~	-
CHY-80-51	2,610.0	448.7	4.7	0.05439	0.00330	0.36200	0.02600	0.04650	0.00160	1.0	313.7	19.0	387.0	130	293.2	9.6	76
CHY-80-52	3,490.0	1,160.0	5.4	0.05380	0.00320	0.35710	0.02500	0.04689	0.00130	1.0	310.0	19.0	362.5	130	295.4	7.9	81
CHY-80-53	4,060.0	1,930.0	4.7	0.05819	0.00350	0.32500	0.02300	0.03982	0.00120	0.9	285.7	18.0	536.0	130	251.7	7.2	47
CHY-80-54	530.9	459.0	1.0	0.06410	0.00410	0.91000	0.09200	0.10130	0.00600	1.0	655.0	49.0	744.0	140	622.0	35.0	84
CHY-80-55	695.0	714.0	0.9	0.05469	0.00330	0.35050	0.02500	0.04552	0.00120	0.8	305.0	19.0	399.0	130	287.0	7.1	72
CHY-80-56	265.8	200.5	1.3	0.05335	0.00320	0.35830	0.02500	0.04747	0.00110	0.9	310.9	19.0	343.0	140	298.9	7.0	87
CHY-80-57	429.0	250.5	1.7	0.05328	0.00320	0.34320	0.02400	0.04583	0.00110	0.8	299.6	18.0	340.5	130	288.8	6.8	85
CHY-80-58	197.9	247.0	0.8	0.08105	0.00480	2.31300	0.16000	0.20290	0.00490	0.7	1,216.2	49.0	1,222.6	120	1,190.7	26.0	97
CHY-80-59	309.0	103.1	3.0	0.08162	0.00490	2.40000	0.17000	0.20960	0.00690	1.0	1,242.0	51.0	1,236.5	120	1,226.0	37.0	99
CHY-80-60	206.1	93.3	2.3	0.07503	0.00450	1.71000	0.12000	0.16370	0.00420	1.0	1,012.3	45.0	1,069.1	120	977.3	23.0	91
CHY-80-61	172.0	58.4	3.1	0.07599	0.00450	1.91200	0.14000	0.17960	0.00610	1.0	1,084.0	50.0	1,094.7	120	1,065.0	33.0	97
CHY-80-62	603.0	185.0	3.7	0.05811	0.00350	0.54300	0.04100	0.06700	0.00310	1.0	441.0	27.0	533.0	130	418.0	19.0	78
CHY-80-63	244.0	28.1	9.8	0.06551	0.00400	0.68400	0.06100	0.07350	0.00330	1.0	528.0	37.0	798.0	110	463.0	23.0	58
CHY-80-64	136.9	102.0	1.5	0.05237	0.00310	0.33300	0.02300	0.04555	0.00110	0.6	291.8	18.0	301.0	140	287.2	6.8	95
CHY-80-65	146.9	137.5	1.2	0.05590	0.00340	0.49770	0.03500	0.06484	0.00160	0.7	410.1	24.0	448.0	130	405.0	9.8	90
CHY-80-66	439.0	264.0	1.8	0.06110	0.00380	0.72300	0.05400	0.08430	0.00350	1.0	552.0	31.0	653.0	150	522.0	21.0	80
CHY-80-67	270.0	73.6	3.8	0.06564	0.00390	1.23700	0.08800	0.13620	0.00380	1.0	817.5	40.0	794.9	120	823.0	22.0	104
CHY-80-68	455.0	109.5	4.2	0.06521	0.00390	1.28200	0.10000	0.14340	0.00690	1.0	837.0	46.0	781.1	130	864.0	39.0	111
CHY-80-69	433.0	268.0	1.6	0.05716	0.00340	0.56800	0.04100	0.07340	0.00220	1.0	456.4	27.0	498.0	130	456.8	13.0	92

Appendix 1a. continued.

SAMPLE CHY-39; 26°23'22.52"S/69°29'13.92"W, h. 2140 m; Analysis at CPGeo, Brazil.

Grain-Spot	Common Pb %	U ppm	Th ppm	Th/U	Pb Rad. ppm	Isotope ratios						Coef. Corr.	Apparent ages (Ma)				Con. %
						$^{238}U/^{206}Pb$	±1σ	$^{207}Pb/^{206}Pb$	±1σ	$^{208}Pb^*/^{206*}Pb$	±1σ		$^{207}Pb^*/^{206}Pb^*$	±1σ	$^{206}Pb^*/^{238}U^*$	±1σ	
CHY39-1.1	0.21	318.9	225.3	0.706	69.7	5.0503	0.0467	0.0754	0.0013	0.2118	0.0069	0.81	1.078	0.035	1.165	0.01	107
CHY39-10.1	0.12	233.1	300.8	1.291	106.9	3.1283	0.0288	0.1179	0.0019	0.3306	0.0233	0.95	1.925	0.029	1.788	0.014	92
CHY39-17.1	0.19	221.6	280.3	1.265	92.8	3.0946	0.0337	0.1086	0.002	0.3612	0.0406	0.9	1.776	0.033	1.805	0.017	101
CHY39-21.1	0.39	120.2	49.6	0.412	26.6	4.8591	0.0637	0.0783	0.0023	0.1115	0.0089	0.19	1.154	0.057	1.206	0.014	104
CHY39-27.1	0.48	276.7	137.6	0.497	63.4	5.1437	0.0655	0.0783	0.0018	0.1724	0.0183	0.8	1.154	0.046	1.145	0.013	99
CHY39-28.1	0.06	733.7	442.8	0.604	175.9	4.7924	0.0496	0.0813	0.0012	0.168	0.0078	1	1.228	0.03	1.222	0.012	99
CHY39-32.1	0.03	2,176	100.7	0.046	1,046.7	2.2069	0.0222	0.1681	0.0021	0.0071	0.0018	0.94	2.539	0.021	2.409	0.02	94
CHY39-38.1	0.09	252.2	129	0.511	217.7	1.5076	0.0142	0.2932	0.0037	0.0467	0.0248	1	3.435	0.02	3.28	0.026	95
CHY39-60.1	2.79	499.6	550.1	1.101	145.2	4.4339	0.0506	0.0872	0.0013	0.2677	0.0613	0.96	1.364	0.03	1.311	0.014	96
CHY39-4.1	0.17	419.6	145.8	0.348	82.4	5.4596	0.0482	0.0757	0.0012	0.1189	0.0076	0.66	1.087	0.032	1.084	0.009	99
CHY39-37.1	0.15	832.4	361.4	0.434	162.9	5.8996	0.061	0.0727	0.0013	0.0973	0.0184	0.91	1.005	0.036	1.009	0.01	100
CHY39-52.1	0.42	162	148.9	0.919	34.9	5.4858	0.1014	0.0752	0.0026	0.1997	0.0465	0.82	1.074	0.068	1.079	0.018	100
CHY39-2.1	1.58	485.5	280.5	0.578	67	7.7003	0.0691	0.065	0.0012	0.1818	0.0048	0.92	0.775	0.038	0.787	0.007	101
CHY39-3.1	0.06	1,057.1	152.6	0.144	114.5	8.9759	0.0728	0.0608	0.0009	0.0318	0.0067	0.85	0.633	0.032	0.681	0.005	107
CHY39-5.1	1.26	820.2	285.1	0.348	63	13.6362	0.3419	0.0586	0.0032	0.0807	0.06	0.61	0.554	0.065	0.456	0.011	82
CHY39-6.1	0.89	309.7	303.7	0.981	29.8	13.5558	0.1616	0.0559	0.0017	0.2735	0.0372	0.7	0.449	0.067	0.459	0.005	102
CHY39-8.1	0.07	733.8	483.3	0.659	65.3	12.9275	0.1138	0.0562	0.0011	0.1425	0.0382	0.98	0.459	0.044	0.48	0.004	104
CHY39-9.1	0	672.8	1,083.5	1.611	94.7	9.6377	0.0878	0.0601	0.0011	0.4096	0.0691	0.38	0.607	0.041	0.636	0.006	104
CHY39-11.1	0.38	442.3	279.6	0.632	40.3	12.6385	0.1351	0.0574	0.0015	0.1652	0.0238	0.75	0.509	0.057	0.491	0.005	96
CHY39-14.1	0.46	557.7	281.2	0.504	32.3	20.0969	0.2494	0.0532	0.0014	0.1305	0.0133	0.91	0.338	0.062	0.313	0.004	92
CHY39-15.1	0.82	285	425.3	1.492	37.3	11.2599	0.1423	0.0587	0.0018	0.4082	0.0393	0.69	0.557	0.067	0.548	0.007	98
CHY39-16.1	5.89	253.9	161.1	0.634	13.7	20.1922	0.3189	0.0529	0.0026	0.8519	4.6316	0.16	0.326	0.112	0.312	0.005	95
CHY39-18.1	0.29	338.9	90.5	0.267	32.9	11.6944	0.1351	0.0588	0.0016	0.0644	0.0126	0.95	0.561	0.057	0.529	0.006	94
CHY39-19.1	0.46	123.8	99.7	0.806	18.9	8.1136	0.1202	0.0642	0.0025	0.2123	0.0308	0.89	0.749	0.081	0.749	0.01	100
CHY39-22.1	0.58	476.7	157.7	0.331	25.6	19.1697	0.2407	0.0534	0.0018	0.1232	0.0147	0.31	0.348	0.077	0.328	0.004	94
CHY39-23.1	2.43	144.4	86.5	0.599	21.5	7.9771	0.1138	0.0645	0.0024	0.1593	0.0193	0.97	0.757	0.08	0.761	0.01	100
CHY39-24.1	0.07	860.1	316.2	0.368	163.2	6.0383	0.0576	0.0739	0.0011	0.1085	0.0018	0.97	1.038	0.031	0.988	0.009	95
CHY39-25.1	0.21	575.4	123.6	0.215	82.5	6.2254	0.0618	0.0711	0.0013	0.0747	0.0074	0.97	0.96	0.037	0.96	0.009	100
CHY39-33.1	1.28	398.7	189	0.474	36.7	11.512	0.1442	0.0584	0.0017	0.1207	0.0207	0.98	0.544	0.066	0.537	0.006	98
CHY39-34.1	1.53	490.9	407.6	0.83	47.9	11.6956	0.1755	0.0573	0.002	0.2249	0.2429	0.93	0.503	0.077	0.529	0.008	105
CHY39-35.1	0.6	1,207.1	854	0.707	86.6	15.5909	0.1748	0.0548	0.0011	0.2051	0.096	0.01	0.404	0.046	0.401	0.004	99
CHY39-40.1	2.79	1,671.9	1,107.8	0.663	191.6	9.0925	0.0949	0.0625	0.0009	0.1216	0.0334	0.99	0.692	0.03	0.673	0.007	97
CHY39-44.1	0.24	1,386.9	983	0.709	87.4	17.2414	0.222	0.0538	0.0011	0.173	0.0254	0.91	0.363	0.047	0.363	0.005	100
CHY39-46.1	0.07	858	736.1	0.858	153.9	7.2085	0.0801	0.0689	0.001	0.2118	0.1049	0.93	0.895	0.032	0.837	0.009	93

Appendix 1a. continued.

Grain-Spot	Common Pb %	U ppm	Th ppm	Th/U	Pb Rad. ppm	Isotope ratios $^{238}U/^{206}Pb$	±1σ	$^{207}Pb/^{206}Pb$	±1σ	$^{208}Pb^*/^{206*}Pb$	±1σ	Coef. Corr.	Apparent ages (Ma) $^{207}Pb^*/^{206}Pb^*$	±1σ	$^{206}Pb^*/^{238}U^*$	±1σ	Con. %
CHY39-48.1	0.02	526.5	118.8	0.226	47.6	11.8961	0.1483	0.0583	0.0013	0.1054	0.1031	0.99	0.539	0.048	0.52	0.006	96
CHY39-49.1	1.2	342.9	65.5	0.191	26.2	14.5752	0.2176	0.055	0.0018	0.0411	0.013	0.88	0.411	0.072	0.428	0.006	104
CHY39-50.1	0.5	763	314.5	0.412	77.1	9.8943	0.1173	0.0598	0.0011	0.1305	0.0599	0.87	0.598	0.038	0.621	0.007	103
CHY39-51.1	0.17	2,677	355.7	0.133	273.5	9.7394	0.0999	0.0606	0.0008	0.0368	0.0027	0.99	0.626	0.028	0.63	0.006	100
CHY39-53.1	0.22	1,554.4	513.1	0.33	167.3	10.0121	0.1033	0.0607	0.0009	0.0693	0.0342	0.01	0.629	0.032	0.614	0.006	97
CHY39-54.1	0.1	1,234.5	322.2	0.261	204.8	6.4345	0.071	0.073	0.0011	0.0782	0.0195	1	1.014	0.029	0.931	0.01	91
CHY39-55.1	0.5	1,147	617.6	0.538	73.4	17.661	0.2199	0.0535	0.0011	0.1631	0.0055	0.43	0.349	0.046	0.355	0.004	101
CHY39-56.1	2.16	920.6	687.4	0.747	92.8	11.6507	0.1367	0.0582	0.0011	0.2133	0.1288	0.68	0.538	0.039	0.531	0.006	98
CHY39-62.1	0.69	566.2	452.9	0.8	51.4	12.4058	0.1608	0.0564	0.0016	0.1419	0.0592	0.98	0.47	0.062	0.5	0.006	106
CHY39-43.1	6.42	1,157.2	536.2	0.463	61.7	20.7302	0.2806	0.0522	0.0013	0.1203	0.1188	0.84	0.292	0.053	0.304	0.004	103
CHY39-7.1	2.04	1,623.3	344.4	0.212	141.2	14.1168	0.1301	0.0579	0.0011	0.0245	0.0053	0.97	0.525	0.039	0.441	0.004	84
CHY39-10.2	0.14	779.3	139.8	0.179	222.9	3.8878	0.0303	0.107	0.0014	0.0324	0.0429	0.98	1.75	0.03	1.476	0.01	84
CHY39-12.1	0.38	535	178.6	0.334	36.9	15.8037	0.1705	0.0559	0.0014	0.1274	0.132	0.77	0.447	0.059	0.396	0.004	88
CHY39-13.1	2.57	808.9	142.8	0.176	58.6	13.0994	0.1304	0.0583	0.0012	0.0367	0.0048	0.99	0.54	0.047	0.474	0.005	87
CHY39-20.1	0.35	798.2	54.8	0.069	112	7.4916	0.069	0.0714	0.0012	0.0156	0.0028	0.99	0.969	0.034	0.808	0.007	83
CHY39-26.1	8.62	1,156.7	435.8	0.377	139.9	8.76	0.0913	0.0718	0.0013	0.0904	0.0085	0.99	0.98	0.037	0.697	0.007	71
CHY39-29.1	11.9	100.3	95.4	0.951	6.6	19.0533	0.6856	0.0563	0.0092	0.279	0.0536	0.51	0.465	0.305	0.33	0.012	70
CHY39-30.1	0	480.5	715.9	1.49	328.1	3.1234	0.0356	0.1566	0.0023	0.1556	0.1496	0.92	2.419	0.026	1.791	0.018	74
CHY39-31.1	0.7	421.6	364.7	0.865	90.3	7.169	0.0791	0.073	0.0013	0.1652	0.0687	0.95	1.015	0.036	0.842	0.009	82
CHY39-36.1	2.57	842.7	222.5	0.264	123	12.2806	0.2163	0.0608	0.0015	0.0548	0.0405	1	0.63	0.051	0.505	0.008	80
CHY39-39.1	1.18	380.5	178.3	0.468	56.7	13.2284	0.1928	0.06	0.0013	0.0844	0.0613	0.78	0.603	0.046	0.47	0.007	77
CHY39-41.1	0.07	529.1	478.1	0.904	64.7	9.0219	0.1218	0.0602	0.0014	0.2358	0.0299	0.91	0.609	0.05	0.678	0.009	111
CHY39-42.1	0.3	740.6	568.5	0.768	142.3	6.2796	0.0687	0.0754	0.001	0.0644	0.0676	0.89	1.078	0.028	0.953	0.01	88
CHY39-44.2	5	1,663.8	933.8	0.561	93	16.4456	0.2054	0.0529	0.0011	0.111	0.0162	0.94	0.326	0.044	0.381	0.005	116
CHY39-45.1	0.76	456.6	-16.3	-0.036	58.3	15.3272	0.3306	0.0499	0.0016	0.0536	0.0863	0.89	0.191	0.063	0.407	0.008	213
CHY39-47.1	2.97	2361.5	1,778.6	0.753	188.8	14.986	0.1643	0.0564	0.0009	0.2184	0.0638	0.89	0.468	0.036	0.416	0.004	89
CHY39-57.1	12.7	200.3	97	0.484	33.1	15.9684	0.2999	0.0603	0.0015	0.1035	0.0357	1	0.613	0.049	0.392	0.007	63
CHY39-58.1	7.47	552.2	434.2	0.786	41.3	15.6713	0.2137	0.0576	0.0017	0.1518	0.0486	0.92	0.514	0.066	0.399	0.005	77
CHY39-59.1	10.39	1,552	399.5	0.257	184.9	10.239	0.1094	0.0631	0.0009	0.062	0.0218	0.67	0.712	0.031	0.601	0.006	84
CHY39-61.1	0.23	1,398.7	22.3	0.016	239.1	7.8063	0.0838	0.0736	0.001	0.0089	0.0083	1	1.029	0.027	0.777	0.008	75
CHY39-63.1	0	154.5	4.4	0.028	40.5	7.2343	0.1051	0.0809	0.0016	0.0124	0.0087	1	1.219	0.037	0.835	0.011	68

CROSS out data = analytically inaccurate; Con. = % of concordance.

APPENDIX 1b. ZIRCON U-PB ANALYTICAL DATA OF GRANITOIDS.

SAMPLE CHY-83 Pink, sheared granite; 25°55'36.50"S/69°19'58.70"W, h. 2868 m; 49 spots; LA-ICP-MS U-Pb age=278.3±5.8 Ma (95% conf.).

Grain-Spot	U ppm	Th ppm	U/Th	Isotope ratios						Error Corr.	Apparent ages (Ma)					
				$^{207}Pb^*/^{206}Pb^*$	±1σ	$^{207}Pb^*/^{235}U^*$	±1σ	$^{206}Pb^*/^{238}U$	±1σ		$^{207}Pb^*/^{235}U$	±1σ	$^{207}Pb^*/^{206}Pb^*$	±1σ	$^{206}Pb^*/^{238}U^*$	±1σ
CHY-83-1	327.6	265.0	1.2	0.0592	0.0050	0.3620	0.0370	0.0440	0.0019	0.9000	311.0	27.0	530	170	277.7	12.0
CHY-83-2	458.6	280.0	1.5	0.0551	0.0045	0.3260	0.0550	0.0423	0.0017	0.9000	316.0	32.0	390	170	267.6	11.0
CHY-83-3	542.0	228.6	2.1	0.0528	0.0036	0.2560	0.0710	0.0434	0.0018	0.9000	231.0	36.0	324	140	274.0	11.0
CHY-83-4	3540.0	687.0	4.6	0.0524	0.0031	0.2940	0.0240	0.0414	0.0017	0.9000	261.4	19.0	289	130	261.5	10.0
CHY-83-5	507.0	282.0	2.4	0.0531	0.0036	0.3310	0.0290	0.0449	0.0019	0.9000	292.3	21.0	326	150	283.3	12.0
CHY-83-6	332.0	363.0	1.3	0.0531	0.0041	0.3400	0.1000	0.0438	0.0018	0.9000	323.0	30.0	320	150	276.3	11.0
CHY-83-7	60.7	57.0	1.4	0.0469	0.0071	0.2740	0.0440	0.0426	0.0020	0.9000	252.0	32.0	120	240	268.9	12.0
CHY-83-8	115.7	84.6	1.3	0.0567	0.0044	0.3450	0.0330	0.0446	0.0019	0.9000	302.0	25.0	440	160	281.2	12.0
CHY-83-9	105.4	53.6	1.7	0.0567	0.0051	0.3400	0.0360	0.0445	0.0019	0.9000	300.0	27.0	450	190	280.3	12.0
CHY-83-10	89.9	66.1	1.2	0.0469	0.0057	0.2820	0.0360	0.0435	0.0020	0.9000	248.0	29.0	50	210	275.3	12.0
CHY-83-11	166.9	99.8	1.4	0.0520	0.0039	0.3970	0.0590	0.0450	0.0019	0.9000	314.0	26.0	310	150	283.8	11.0
CHY-83-12	153.2	95.4	1.5	0.0541	0.0044	0.3220	0.0320	0.0432	0.0018	0.9000	282.0	25.0	350	170	272.4	11.0
CHY-83-13	346.0	704.0	1.8	0.0531	0.0041	0.3100	0.0300	0.0419	0.0017	0.9000	274.0	23.0	300	160	264.9	11.0
CHY-83-14	147.1	358.3	1.4	0.0514	0.0052	0.3200	0.0360	0.0446	0.0019	0.9000	285.0	28.0	240	190	281.5	12.0
CHY-83-15	287.0	423.0	2.2	0.0574	0.0043	0.3440	0.0320	0.0446	0.0019	0.9000	297.0	25.0	450	160	281.5	11.0
CHY-83-16	176.2	173.9	1.7	0.0540	0.0055	0.3180	0.0360	0.0435	0.0018	0.9000	279.0	28.0	290	190	274.5	11.0
CHY-83-17	184.7	159.7	1.6	0.0545	0.0042	0.3040	0.0290	0.0410	0.0017	0.9000	269.0	22.0	370	160	259.1	11.0
CHY-83-18	706.0	224.6	2.8	0.0540	0.0039	0.3500	0.1300	0.0421	0.0017	0.9000	330.0	66.0	370	160	266.1	11.0
CHY-83-19	119.0	46.1	2.0	0.0563	0.0064	0.3250	0.0390	0.0432	0.0019	0.9000	293.0	31.0	410	210	272.5	12.0
CHY-83-20	340.2	117.2	2.3	0.0505	0.0040	0.3090	0.0300	0.0440	0.0018	0.9000	272.0	23.0	200	160	277.4	11.0
CHY-83-21	351.0	108.8	2.5	0.0515	0.0040	0.3070	0.0290	0.0430	0.0017	0.9000	274.0	23.0	260	160	271.5	11.0
CHY-83-22	177.8	97.6	1.3	0.0563	0.0042	0.3450	0.0330	0.0440	0.0018	0.9000	301.0	25.0	450	150	277.4	11.0
CHY-83-23	295.3	185.7	1.2	0.0506	0.0040	0.3060	0.0290	0.0444	0.0018	0.9000	270.0	23.0	200	160	279.9	11.0
CHY-83-24	303.7	102.5	2.3	0.0546	0.0041	0.3430	0.0630	0.0436	0.0018	0.9000	311.0	24.0	350	150	275.3	11.0
CHY-83-25	261.0	116.0	1.9	0.0528	0.0039	0.3290	0.0780	0.0438	0.0018	0.9000	317.0	35.0	300	150	276.2	11.0
CHY-83-26	256.0	123.1	1.7	0.0544	0.0048	0.3090	0.0320	0.0412	0.0017	0.9000	271.0	25.0	340	180	260.0	11.0
CHY-83-27	135.5	49.0	2.4	0.0495	0.0047	0.3190	0.0340	0.0464	0.0020	0.9000	281.0	27.0	210	180	292.5	12.0
CHY-83-28	472.0	132.8	3.2	0.0517	0.0038	0.3100	0.0290	0.0434	0.0018	0.9000	274.0	22.0	255	150	273.5	11.0
CHY-83-29	416.0	183.0	2.4	0.0604	0.0046	0.3050	0.0900	0.0449	0.0018	0.9000	243.0	53.0	580	160	282.8	11.0
CHY-83-30	499.0	175.9	2.8	0.0492	0.0041	0.2690	0.1000	0.0430	0.0018	0.9000	259.0	62.0	180	170	271.1	11.0
CHY-83-31	191.0	104.0	2.2	0.0532	0.0046	0.3080	0.0320	0.0425	0.0019	0.9000	272.0	25.0	310	180	268.2	12.0
CHY-83-32	933.0	526.9	1.9	0.0545	0.0034	0.3251	0.0270	0.0438	0.0018	0.9000	285.3	21.0	387	140	276.4	11.0
CHY-83-33	554.0	310.3	1.9	0.0603	0.0042	0.3590	0.0320	0.0409	0.0016	0.9000	311.0	24.0	605	150	258.3	10.0
CHY-83-34	370.0	207.0	1.9	0.0519	0.0043	0.3380	0.0340	0.0437	0.0018	0.9000	294.0	26.0	290	170	275.9	11.0
CHY-83-35	451.0	298.6	1.6	0.0579	0.0040	0.3160	0.0800	0.0425	0.0017	0.9000	299.0	34.0	513	150	268.3	11.0
CHY-83-36	579.3	224.0	2.7	0.0551	0.0036	0.3960	0.0630	0.0425	0.0017	0.9000	300.0	19.0	396	140	268.3	10.0

Appendix 1b. continued.

Grain-Spot	U ppm	Th ppm	U/Th	Isotope ratios						Error Corr.	Apparent ages (Ma)					
				$^{207}Pb^*/^{206}Pb^*$	±1σ	$^{207}Pb^*/^{235}U^*$	±1σ	$^{206}Pb^*/^{238}U$	±1σ		$^{207}Pb^*/^{235}U$	±1σ	$^{207}Pb^*/^{206}Pb^*$	±1σ	$^{206}Pb^*/^{238}U^*$	±1σ
CHY-83-37	581.0	284.0	2.1	0.0544	0.0036	0.3080	0.0270	0.0411	0.0017	0.9000	273.2	21.0	367	140	259.7	10.0
CHY-83-38	302.0	120.0	2.5	0.0569	0.0041	0.2500	0.1000	0.0458	0.0019	0.9000	234.0	66.0	473	150	288.9	12.0
CHY-83-39	53.2	23.1	2.3	0.0487	0.0062	0.2890	0.0390	0.0438	0.0021	0.9000	252.0	31.0	90	230	276.0	13.0
CHY-83-40	136.8	68.8	2.0	0.0510	0.0040	0.3290	0.0330	0.0432	0.0018	0.9000	285.0	25.0	220	150	272.3	11.0
CHY-83-41	255.9	89.0	2.9	0.0535	0.0041	0.3270	0.0320	0.0433	0.0018	0.9000	285.0	24.0	330	150	273.0	11.0
CHY-83-42	274.6	91.0	3.0	0.0510	0.0040	0.3410	0.0340	0.0437	0.0018	0.9000	296.0	26.0	260	170	275.8	11.0
CHY-83-43	205.0	109.0	1.9	0.0515	0.0042	0.2800	0.1100	0.0426	0.0019	0.9000	303.0	52.0	240	160	269.1	12.0
CHY-83-44	178.8	99.6	1.8	0.0554	0.0056	0.3740	0.0450	0.0426	0.0019	0.9000	325.0	31.0	400	210	268.7	12.0
CHY-83-45	317.0	119.9	2.6	0.0609	0.0046	0.3840	0.0370	0.0441	0.0020	0.9000	330.0	26.0	610	160	278.0	12.0
CHY-83-46	495.0	173.0	2.7	0.0544	0.0035	0.3370	0.0290	0.0449	0.0018	0.9000	294.5	22.0	363	140	282.9	11.0
CHY-83-47	178.5	60.2	2.8	0.0523	0.0054	0.3280	0.0360	0.0449	0.0020	0.9000	289.0	27.0	350	210	283.0	13.0
CHY-83-48	349.0	148.7	2.1	0.0530	0.0039	0.3610	0.0430	0.0421	0.0017	0.9000	303.0	26.0	320	150	266.1	11.0
CHY-83-49	1089.0	345.0	2.9	0.0544	0.0036	0.3580	0.0320	0.0481	0.0021	0.9000	313.0	25.0	370	150	302.9	13.0
CHY-83-50	334.0	287.6	1.1	0.0545	0.0047	0.3440	0.0350	0.0466	0.0021	0.9000	296.0	26.0	350	170	293.6	13.0
CHY-83-51	615.0	492.0	1.3	0.0543	0.0043	0.3440	0.0320	0.0437	0.0018	0.9000	301.0	25.0	370	160	275.6	11.0
CHY-83-52	1591.0	956.0	1.8	0.0538	0.0034	0.2030	0.1000	0.0420	0.0017	0.9000	212.0	49.0	356	140	264.9	10.0

SAMPLE CHY-74; Pink granite; 26°23'23.18"S/69°29'13.81"W, h. 2138 m; 6 spots; LA-ICP-MS U-Pb age = 292.2±6.6 Ma (95% conf.).

Grain-Spot	U ppm	Th ppm	U/Th	Isotope ratios						Error Corr.	Apparent ages (Ma)					
				$^{207}Pb^*/^{206}Pb^*$	±1σ	$^{207}Pb^*/^{235}U^*$	±1σ	$^{206}Pb^*/^{238}U$	±1σ		$^{207}Pb^*/^{235}U$	±1σ	$^{207}Pb^*/^{206}Pb^*$	±1σ	$^{206}Pb^*/^{238}U^*$	±1σ
CHY-74-1	970.0	395.0	2.5	0.05329	0.00140	0.35000	0.02000	0.04800	0.00290	1.0	305.0	15.0	340.9	60	302.0	18.0
CHY-74-2	1056.0	681.0	1.6	0.05116	0.00140	0.33340	0.00570	0.04714	0.00110	0.8	292.2	4.4	248.0	63	297.0	6.6
CHY-74-3	667.0	450.0	1.5	0.05070	0.00130	0.34700	0.00640	0.04938	0.00110	0.8	302.5	4.9	227.0	63	310.7	7.0
CHY-74-4	764.0	80.1	9.5	0.05565	0.00150	0.42030	0.00790	0.05460	0.00130	0.8	356.3	5.6	438.0	61	342.7	7.7
CHY-74-5	777.0	82.1	9.4	0.05393	0.00140	0.40070	0.00700	0.05348	0.00120	0.3	342.2	5.1	368.0	61	335.9	7.4
CHY-74-6	154.5	83.8	1.8	0.05699	0.00150	0.70150	0.01300	0.08929	0.00200	0.8	539.7	7.5	491.0	59	551.3	12.0
CHY-74-7	610.0	383.0	1.6	0.05114	0.00140	0.33100	0.00690	0.04705	0.00120	0.9	290.3	5.2	250.0	69	296.4	7.2
CHY-74-8	550.0	273.0	2.0	0.05157	0.00140	0.32620	0.00630	0.04615	0.00110	1.0	286.6	4.8	266.5	62	290.8	7.0
CHY-74-9	1335.0	860.0	1.5	0.05286	0.00140	0.32690	0.00590	0.04515	0.00100	0.9	287.2	4.5	322.6	60	284.7	6.3
CHY-74-10	367.0	197.0	1.8	0.06169	0.00160	0.92050	0.01700	0.10879	0.00250	0.9	662.6	8.8	663.4	57	665.7	14.0
CHY-74-11	226.0	45.6	5.2	0.05991	0.00160	0.79450	0.01400	0.09618	0.00220	0.8	593.7	7.9	600.2	57	592.0	13.0
CHY-74-12	275.3	123.5	2.2	0.05999	0.00160	0.78580	0.01500	0.09500	0.00230	1.0	588.7	8.5	603.1	57	585.0	13.0
CHY-74-13	541.0	299.0	1.8	0.05754	0.00150	0.62000	0.01000	0.07819	0.00170	0.6	489.8	6.5	512.1	58	485.3	10.0
CHY-74-14	482.0	133.0	4.3	0.05978	0.00160	0.74400	0.01600	0.09040	0.00230	1.0	565.0	9.6	596.0	58	557.8	13.0
CHY-74-15	192.4	439.0	0.4	0.05965	0.00160	0.80820	0.01400	0.09865	0.00220	0.7	601.4	7.7	590.8	58	606.5	13.0
CHY-74-16	329.0	146.0	2.2	0.05629	0.00150	0.58850	0.01200	0.07574	0.00180	0.9	469.9	7.7	463.9	59	470.6	11.0
CHY-74-17	516.0	116.3	4.4	0.05812	0.00150	0.66400	0.02800	0.08240	0.00370	1.0	517.0	17.0	534.3	58	511.0	22.0

Appendix 2b. continued.

SAMPLE CHY-19a; Dark green, foliated tonalite; 26°23'22.05"S/69°29'09.62"W, h. 2134 m; 14 spots; SHRIMP U-Pb age = 285.7±6.8 Ma (95% conf.).

Grain Spot	Common ^{206}Pb %	U ppm	Th ppm	$^{232}Th/^{238}U$	Radiogenic ^{206}Pb ppm	$^{204}Pb/^{206}Pb$	Total $^{238}U/^{206}Pb$	Error %	Total $^{207}Pb/^{206}Pb$	Error %	Radiogenic $^{238}U/^{206}Pb$	Error %	Radiogenic $^{207}Pb/^{206}Pb$	Error %	^{204}Pb corrected $^{206}Pb/^{238}U$ Age Ma	Error ±1σ
CHY19A-1.1	0.47	276.45	215.44	0.81	11.16	0.000259	21.28	4.75	0.056364	2.34	21.38	4.75	0.05257	3.36	294.7	13.7
CHY19A-2.1	2.02	244.59	54.50	0.23	9.97	0.001109	21.08	4.27	0.072065	6.10	21.51	4.37	0.05589	16.09	292.8	12.5
CHY19A-3.1	0.09	1,461.19	21.54	0.02	55.01	0.000049	22.82	4.75	0.051257	1.19	22.84	4.75	0.05053	1.23	276.2	12.9
CHY19A-4.1	0.44	604.21	42.02	0.07	23.33	0.000243	22.25	8.34	0.053948	1.73	22.35	8.34	0.05037	2.78	282.1	23.0
CHY19A-5.1	-0.02	538.56	628.46	1.21	21.87	-0.000009	21.16	4.22	0.052540	1.77	21.15	4.22	0.05267	1.78	297.7	12.3
CHY19A-6.1	0.01	459.58	258.62	0.58	17.78	0.000005	22.21	4.44	0.054340	1.84	22.21	4.44	0.05426	2.26	283.9	12.3
CHY19A-7.1	0.11	1.230.06	315.62	0.27	49.14	0.000061	21.50	4.29	0.053051	1.16	21.53	4.29	0.05216	1.43	292.7	12.3
CHY19A-8.1	0.35	364.00	300.98	0.85	14.58	0.000190	21.44	4.23	0.055675	2.78	21.52	4.23	0.05289	3.34	292.8	12.1
CHY19A-9.1	0.55	256.71	128.25	0.52	9.94	0.000301	22.19	4.26	0.056154	2.40	22.31	4.28	0.05173	6.90	282.6	11.8
CHY19A-10.1	-0.03	2.520.25	451.11	0.18	98.89	-0.000019	21.89	4.19	0.052062	0.80	21.89	4.19	0.05233	0.80	288.0	11.8
CHY19A-11.1	0.44	398.18	244.23	0.63	16.04	0.000241	21.33	4.24	0.055656	2.15	21.43	4.24	0.05212	3.75	294.0	12.2
CHY19A-12.1	0.07	981.44	31.23	0.03	37.02	0.000041	22.78	4.19	0.052207	1.59	22.79	4.19	0.05161	1.68	276.8	11.3
CHY19A-13.1	0.20	801.68	27.43	0.04	30.28	0.000110	22.74	4.20	0.053643	1.41	22.79	4.20	0.05202	2.08	276.8	11.4
CHY19A-14.1	2.25	278.91	185.59	0.69	10.46	0.001228	22.90	5.27	0.069662	2.09	23.43	5.34	0.05165	13.87	269.3	14.1